A TIME-DEPENDENT STUDY OF BISTABILITY IN RESONANT TUNNELING STRUCTURES

A THESIS

SUBMITTED TO THE DEPARTMENT OF PHYSICS

AND THE INSTITUTE OF ENGINEERING AND SCIENCE

OF BILKENT UNIVERSITY

IN PARTIAL FULFILLMENT OF THE REQUIREMENTS

FOR THE DEGREE OF

MASTER OF SCIENCE

By

Ersin Kocacioğlu

August 1997

A TIME-DEPENDENT STUDY OF BISTABILITY IN RESONANT TUNNELING STRUCTURES

A THESIS

SUBMITTED TO THE DEPARTMENT OF PHYSICS

AND THE INSTITUTE OF ENGINEERING AND SCIENCE

OF BİLKENT UNIVERSITY

IN PARTIAL FULFILLMENT OF THE REQUIREMENTS

FOR THE DEGREE OF

MASTER OF SCIENCE

Ersin Kececioglu

By

Ersin Keçecioğlu

August 1997

I certify that I have read this thesis and that in my opinion it is fully adequate, in scope and in quality, as a dissertation for the degree of Master of Science.

Prof. M. Cemal Yalabık (Supervisor)

I certify that I have read this thesis and that in my opinion it is fully adequate, in scope and in quality, as a dissertation for the degree of Master of Science.

Assoc. Prof. Ekmel Özbay

I certify that I have read this thesis and that in my opinion it is fully adequate, in scope and in quality, as a dissertation for the degree of Master of Science.

Assoc. Prof. Bilal Tanatar

Approved for the Institute of Engineering and Science:

Prof. Mehmet Baray,
Director of Institute of Engineering and Science

Abstract

A TIME-DEPENDENT STUDY OF BISTABILITY IN RESONANT TUNNELING STRUCTURES

Ersin Keçecioğlu
M. S. in Physics
Supervisor: Prof. M. Cemal Yalabık
August 1997

A computational time-dependent study of the bistability in resonant tunneling structures including the electron-electron interactions is presented. A new computational method for the investigation of many particle interacting systems for the study of quantum transport in small systems is introduced. The time-dependence of the wave-function in the Schrödinger equation is studied by discretizing the energy spectrum and the time steps.

A simple model for a double barrier resonant tunneling structure is introduced. The method is then applied to this simple model of double barrier resonant tunneling structure, and this geometry is investigated systematically in terms of inter-particle interaction strength and number of particles. By applying the method to this simple geometry it is shown that there exists instabilities which occur as oscillations in the current-voltage characteristics of the model geometry.

Keywords:

Mesoscopics, bistability, Schrödinger equation, numerical solution, time-dependence, quantum transport, double barrier, resonant tunneling, electron-electron interaction, many particle solution

Özet

REZONANT TÜNELLEME YAPILARINDAKİ
ÇİFT-KARARLILIĞIN ZAMANA BAĞLI BİR ÇALIŞMASI

Ersin Keçecioğlu
Fizik Yüksek Lisans
Tez Yöneticisi: Prof. M. Cemal Yalabık
Ağustos 1997

Resonant tünelleme yapılarında görülen çift-kararlılığın elektron-elektron etkileşmelerini içeren, zamana bağlı hesapsal bir çalışması yapıldı. Bu amaç doğrultusunda, küçük sistemlerde kuvantum iletimi, etkileşen çok parçacık sistemlerde analiz edebilmek için hesaba dayalı bir yöntem önerildi. Yöntem en basit haliyle Hamilton fonksiyonun spektrumunun ve zaman basamaklarının süreklilikten kademeli hale dönüştürülmesine dayanıyor.

Çift engelli resonant tünelleme yapıları için basit bir model tanıtıldı. Metod daha sonra, önerilen bu basit modele uygulandı. Çift engelli resonant tünellme yapıları sistematik olarak parçacıklar arası etkileşimin büyüklüğü ve parçacık sayısı değiştirilerek incelendi. Bu incelemeler sonucunda, resonant tünelleme yapılarında kararsızlıklar olduğu ve bunun akım-voltaj eğrilerinde salınımlar

olarak ortaya çıktığı gösterildi.

Anahtar sözcükler: Mezoskopik Fizik, çift-kararlılık,Schrödinger denklemi, numerik çözüm, zamana bağlılık, kuvantum iletim, çift engel, rezonant tünelleme, elektron-elektron etkileşmesi, çok parçacık çözüm

Acknowledgement

It is my pleasure to acknowlege Prof. M. C. Yalabık, my thesis supervisor, for his advice, guidance and understanding throughout my studies. I learned well from him. His special guidance for computational problems helped me very much when I was in panic. He was always understanding also when I could not finish some work in time. During this study, he gave me a hand when I was almost lost.

My special thanks are for E. Tekin, A. Oktay, E. Voyvoda, E. Tekeşin, M. Temizsoy and E. Ofli who were always with me during the last two years of my life. We shared many things. Life could not be easy in Bilkent without them. They always encouraged me in doing physics.

I also would like to thank F. Çelikler, my bridge partner, who was always understanding. I would also like to thank all the research assistants in the department, they were always helpful not especially for me but for everbody, but my special thanks are for H. Boyacı who helped in solving my computer based problems, and B. E. Sağol who was a good partner for free times in Bilkent.

My apartment partner and previous roommate A. Bek deserves special thanks for many things but especially for his good meals. Also my thanks for K. Akalın with whom I spared many funny hours, M. Bayındır who always helped me in latex related problems and my undergraduate classmates D. Vardar and G. Ulu for their morale support from the United States about how I can be a good physicist in Turkey.,

Contents

List of Figures

List of Tables

Chapter 1

INTRODUCTION

In the last few decades micro-fabrication technology has developed rapidly. Due to this growth, new devices with very small dimensions down to a few hundred angstroms have been made. As the dimensions of the devices are reduced, quantum mechanical analysis of them became of vital importance. These devices exhibit many quantum mechanical features in their transport properties. Theoretical models are not easily applicable to all practical systems because of the complexity arising from the many particle feature of the systems. Computational methods on the other hand seem to provide an easy tool especially with the availability of fast and powerful computers.

An interesting structure that has attracted interest is resonant tunneling diode[1–3]. Resonant tunneling structures have been studied for the last $20 - 25$ years, and have been modeled in several ways. Bistability [4,5] that is seen both experimentally and theoretically in these structures is interesting because the quantum mechanical study should provide only one solution with the given boundary conditions. Although this bistable behavior may be studied easily with mean-field approximation, our interest in this work is focused on the appearance of this effect from the linear quantum mechanical treatment. We tried to understand this bistable behavior, in a full quantum mechanical treatment, with the aid of computational methods.

As the feature sizes of fabricated geometries are reduced [6–8], some important

length scales [9] should be compared, which determines the type of transport that describes the motion of carriers in these structures. Three important characteristic lengths are:

1. De Broglie wavelength, which is related to the kinetic energy of the electrons.

2. Mean free path, which is the distance that an electron travels before its initial momentum is destroyed.

3. Phase coherence length, which is the length that an electron does not lose its phase information.

One can relate the coherence length (L_ϕ), to the inelastic mean free time (τ_{in}) via the equation [10]

$$L_\phi = \sqrt{D\tau_{in}} \tag{1.1}$$

where D is the carrier diffusion constant.

A conductor usually shows ohmic characteristics if its dimensions are much larger than these three length scales. This can be called the classical region. In the classical region, the motion of electrons in external fields is described by the Boltzmann transport equation [11].

Recent devices are called mesoscopic, whose dimensions are much larger than microscopic objects such as atoms, but not large enough to be ohmic. Mesoscopic devices, their production technology, and their physics have been extensively studied at low temperatures, and these works have been reviewed extensively [12–15].

Quantum effects are quite significant in mesoscopic devices. Typical examples are conductance fluctuations [16,17], the Aharonov-Bohm oscillations [18,19], and the Coulomb-blockade effect [20]. There is evidence from these ultra-submicron devices that have been fabricated that quantum effects will dominate in future electronic devices. It is clear that as the dimensions of the devices are reduced, quantum mechanical analysis of them become more and more important. It

appears that modeling of new devices should include more detailed quantum contributions [21].

In the last 50 years there were many attempts to form a quantum theory of transport [22–24]. There are mainly two approaches. First one is the Kubo's linear response theory [25,26] which claims that the current is accumulation of the local linear response of the system to an Electro-magnetic field. The other is the Landauer scattering formalism [27,28], which is called Landauer-Büttiker after the works of Büttiker [29–31]. These are powerful methods, but because of the many particle features of the system they are not easily applicable to all systems of interest. Kubo's linear response theory is a powerful tool for infinite systems, but for mesoscopic systems it has some complications. Other than these formalisms, there are also non-equilibrium formalisms of the quantum transport formulated by Keldysh [36] and, Kadanoff and Baym [37] independently. In Chapter 2, quantum transport theories are explained briefly.

On the other hand, computational methods play an important role in modeling and analyzing mesoscopic structures. In Chapter 3, a numerical approach based on the dicretization of the spectrum of the non-interacting Hamiltonian is introduced. Time-dependence is accomplished by again discretizing the time steps. A simple model for the resonant tunneling structures is introduced in Chapter 4 and this computational method is applied to the model. In particular, the behavior of the system under the conditions where bistability is expected (from the mean-field approximation) is studied in detail. Oscillations in the current-voltage characteristics is observed as a consequence of instabilities in the resonant tunneling structures.

Chapter 2

GENERAL QUANTUM TRANSPORT PROBLEM

In quantum transport theory, the general system to be solved may be described by some time-independent Hamiltonian H^0 to which a perturbation (usually external) H^1 is applied. In this case the equation to be solved is the well known Schrödinger equation :

$$[H^0 + H^1]\psi = i\hbar\frac{\partial\psi}{\partial t} \tag{2.1}$$

where $\hbar$ is the Planck's constant divided by 2π.

For time-independent perturbations, Eq. 2.1 reduces to :

$$[H^0 + H^1]\psi = E\psi. \tag{2.2}$$

This form of Eq. 2.2 except the H^1 part is dissipationless, since H^0 is considered to consist of the kinetic part, plus at most an an applied electrostatic potential.

To use the Schrödinger equation directly, if one does not want to lose physical information on the system, it should be assumed that the length scale of the geometry for which Eq. 2.2 is being solved, is smaller than any characteristic dissipation length.

The treatment of transport with the Schrödinger equation (Eq. 2.1 or Eq. 2.2) has followed several approaches. There are mainly two different approaches for

the transport in quantum systems. Basically these are linear response theory introduced by Kubo [25], who argues that the current is the response of the external field, and the scattering formalism introduced by Landauer [27] and Büttiker [29], which governs current as a scattering event of particles over the structure under investigation. In this chapter those approaches based on the Schrödinger equation as well as some other quantum mechanical approaches will be explained.

2.1 Linear Response Theory

In the Kubo's linear response theory [25] approach, total Hamiltonian is divided into two parts as follows :

$$H = H^0 + H^1(t) \tag{2.3}$$

where H is the total Hamiltonian, H^0 includes the electron, lattice, and interaction terms, and H^1 includes the perturbing potential. The current response of the system is incorporated via the vector potential $\mathbf{A}(\mathbf{r}, t)$ as

$$H^1(t) = \int d\mathbf{r}\mathbf{A}(\mathbf{r}, t)\mathbf{j}(\mathbf{r}). \tag{2.4}$$

Here $\mathbf{j}(\mathbf{r})$ is the paramagnetic part of the symmetrized total current operator $\mathbf{J}(\mathbf{r}, t)$

$$\mathbf{J}(\mathbf{r}, t) = \mathbf{j}(\mathbf{r}) - \frac{ne^2}{m}\mathbf{A}(\mathbf{r}, t). \tag{2.5}$$

The formulation of the current reduces to

$$J_\alpha(\mathbf{r}) = \sum_\beta \int d\mathbf{r}\sigma_{\alpha,\beta}E_\beta(\mathbf{r}). \tag{2.6}$$

Here α, β are cartesian coordinates, E is the local electric field due to external field, J is the current density, and σ is the local conductivity tensor.

Kubo formalism is good for infinite systems, but for especially finite small systems it brings complications since the local conductivity tensor σ should be calculated for each structure under investigation, which is complicated, even not possible analytically for most of the geometries.

2.2 Landauer Formula

In the ballistic regime of transport (when the dimensions of the system are smaller than the phase coherence length), the solution of the Schrödinger equation is sufficient to explain all physical quantities. Consider a 1-dimensional quantum structure connected to two reservoirs of chemical potentials μ_{left} and μ_{right} corresponding to left and right reservoirs respectively. The potential difference between two reservoirs is then given by

$$eV = \mu_{left} - \mu_{right} \tag{2.7}$$

where e is the charge of the carriers and V is the potential difference between two reservoirs, correspondingly potential drop over the structure.

The wave-function at the left and right boundaries may be expressed as :

$$\psi(x) = Ae^{ik_l x} + Re^{-ik_l x} \qquad \text{left boundary}$$

$$\psi(x) = Te^{ik_r x} \qquad \text{right boundary.}$$

For a unit incidence i.e., $A = 1$, the other two coefficients R and T can be uniquely determined for any type of potential in the quantum system. The transmission probability, $T_{i\rightarrow j}$ from the injected state i to the transmitted state j can now be determined using this solution. Then total current flowing from left reservoir to the right reservoir can be expressed as the Landauer [27] formula

$$I_{\rightarrow} = \sum_{i,j} F_i e \frac{\hbar k_i}{m} T_{i\rightarrow j} \tag{2.8}$$

where F_i is the distribution function of carriers in the left reservoir. For an electronic system Fermi-Dirac distribution function is used. The term $e\hbar k_i/m$ is the current carried by state i. Total current can be expressed as the current flowing from the left reservoir to the right, minus the current flowing from the right to the left.

Consider a system at zero temperature, so that the states of the reservoirs are filled up to corresponding Fermi energy, and assume that the potential difference

is small so that μ_{left} and μ_{right} do not differ much, and in this region $T_{i\to j}$'s are almost equal to some T. Then total current can be written as:

$$I = \sum_{\sqrt{2m\mu_{right}}/\hbar}^{\sqrt{2m\mu_{left}}/\hbar} e\frac{\hbar k_i}{m}T$$

$$I = \frac{2e}{h}(\mu_{left} - \mu_{right})T = \frac{2e^2}{h}TV. \tag{2.9}$$

A universal conductance of $\frac{2e^2}{h}$ as seen may be calculated.

2.3 Density Matrix

When the system of interest is represented by some state vector $|\phi>$ in some representation, the density matrix is defined as :

$$\rho = |\phi><\phi|. \tag{2.10}$$

Any physical quantity that is represented by the operator A, has the mean value in state $|\phi>$

$$<A>=<\phi|A|\phi>=\sum_{m,n}<\phi|m><m|A|n><n|\phi>$$

$$=\sum_{m,n}\rho_{nm}A_{mn} = Tr(\rho A) \tag{2.11}$$

where ρ_{nm} and A_{mn} are matrix elements of ρ and A respectively.

Beginning from the time-dependent Schrödinger equation (Eq. 2.1), it can be shown that density matrix ρ satisfies the following time-dependent equation

$$i\hbar\frac{d\rho}{dt} = [H, \rho] \tag{2.12}$$

where H is the total Hamiltonian of the system and square brackets means commutator of H and ρ. Then regardless of the type of terms in the Hamiltonian, ρ can be calculated at any time, at least numerically, when the solution at some time $t = t_0$ is known. The dissipative terms in the Hamiltonian may be treated

using perturbative methods. In fact this is a viable method of treating irreversible transport, as has been discussed elsewhere [32–34].

A problem with the density matrix is that it is defined in the position space, with the important quantum effects occurring between two separated points in space. Many problems can be investigated better in a phase space representation, such as electron-electron, electron-phonon etc., interactions, and are difficult with the density matrix representation. It is possible to rearrange the variables so that a phase space representation is feasible [35,40].

2.4 Wigner Functions

The Wigner function [35] may be thought as an extension of the classical distribution function. If we consider, for simplicity, a 1-dimensional system with canonical variables q and p, it is clear that it is not possible to construct a quantum mechanical probability distribution function $P(q,p)$ strictly, such that $P(q,p)dqdp$ is equal to the probability of finding the system in dq around q and dp around p, since this probability is not well defined in quantum mechanics because of Heisenberg uncertainty relations and incompatibility of two canonical variable measurements.

A distribution function which is purely quantum mechanical can be defined as follows:

$$f(x,p,t) = \frac{1}{2\pi\hbar}\int_{-\infty}^{\infty} \psi^*(x-\frac{R}{2},t)\psi(x+\frac{R}{2},t)exp(-\frac{1}{\hbar}Rp)dR. \tag{2.13}$$

This is the Wigner function defined in 1-d, but generalizations to higher dimensions is straightforward. Here ψ is the wave-function, x and t are position and time variables respectively, and p can be thought as the momentum variable.

Some results that follows from Eq. 2.13 are:

$$\int_{-\infty}^{\infty} f(x,p)dp = \psi^*(x)\psi(x) \tag{2.14}$$

$$\int_{-\infty}^{\infty} f(x,p)dx = \varphi^*(p)\varphi(p) \tag{2.15}$$

$$\int\int xf(x,p)dxdp =< x > \tag{2.16}$$

$$\int\int pf(x,p)dxdp =< p > \tag{2.17}$$

with the definition of $\varphi(p)$ as :

$$\varphi(p) = \int \psi(x)exp(-\frac{1}{\hbar}px)dx. \tag{2.18}$$

Then any observable A, which is a function of x and p may be written as :

$$< A >= \int\int A(x,p)f(x,p)dqdp. \tag{2.19}$$

An equation of motion for f may be obtained, which reads in powers of $\hbar$:

$$\frac{\partial f}{\partial t} = -\frac{p}{m}\frac{\partial f}{\partial x} - \frac{\partial V}{\partial x}\frac{\partial f}{\partial p} + \hbar\cdots \tag{2.20}$$

which looks like the classical Boltzmann equation with no collision, when $\hbar$ is set to zero.

This function f can be modified for use as density matrix in phase space.

2.5 Green's Functions

Green's function is a non-equilibrium theory of quantum transport which have been formulated by Keldysh [36] and, Kadanoff and Baym [37] independently. These two formalisms are equivalent but there are some formal differences. Using these formalisms a quantum transport equation can be found [36,37]. Green's functions satisfy the Schrödinger equation in the following form

$$i\hbar\frac{\partial G}{\partial t} - H_0 G = \delta(x - x_1)\delta(t - t_2) \tag{2.21}$$

which was shown elsewhere [36,38,39].

Suppose that we know that a system is formed by a particle that is in x_1 at time t_1, in the Heisenberg representation this state is given by the vector $\Psi^\dagger(x_1,t_1)|0_H >$. Then the probability of finding the particle in x_2 at time t_2 can be written as :

$$< 0_H|\Psi(x_2,t_2)\Psi^\dagger(x_1,t_1)|0_H > . \tag{2.22}$$

This is the basic concept of the definition of Green's function, more precisely, which is defined as :

$$G(x_2,t_2;x_1,t_1) =< \phi_H|\Psi(x_2,t_2)\Psi^\dagger(x_1,t_1)|\phi_H > . \tag{2.23}$$

Here addition of an extra particle to a many body state $|\phi >$ is being considered. This is only one of the Green's functions. We need to define six different Green's functions for a non-equilibrium system. These are advanced G^a, retarded G^r, time ordered G_t, anti-time ordered G_t^-, and $G^>$ and $G^<$, which have no names.

$$G^>(x_1,x_2) = -i < \psi(x_1)\psi^\dagger(x_2) > \tag{2.24}$$

$$G^>(x_1,x_2) = -i < \psi^\dagger(x_2)\psi(x_1) > \tag{2.25}$$

$$G_t(x_1,x_2) = \Theta(t_1-t_2)G^>(x_1,x_2) + \Theta(t_2-t_1)G^<(x_1,x_2) \tag{2.26}$$

$$G_t^-(x_1,x_2) = \Theta(t_2-t_1)G^>(x_1,x_2) + \Theta(t_1-t_2)G^<(x_1,x_2) \tag{2.27}$$

$$G^r(x_1,x_2) = G_t - G^< \tag{2.28}$$

$$G^a(x_1,x_2) = G_t - G^>. \tag{2.29}$$

In these definitions $\psi(x)$ is the field operator defined by the relation :

$$\psi(x) = \sum_i c_i\psi_i(x)exp(-\frac{iE_i}{t}) \tag{2.30}$$

and c_i is the annihilation operator, E_i and ψ_i are the solutions of the eigenvalue equation :

$$H\psi_i(x) = E_i\psi_i(x) \tag{2.31}$$

H being the Hamiltonian of the system.

Furthermore a quantum Boltzmann equation may be constructed using Green's functions [36,37,39].

Chapter 3

THE METHOD AND THE TIME-DEPENDENT ALGORITHM

3.1 Introduction

A most general approach to the quantum transport problem may start with the N-particle, time-dependent Schrödinger equation :

$$H\Psi(x_1, x_2, \cdots, x_N, t) = i\hbar \frac{\partial \Psi(x_1, x_2, \cdots, x_N, t)}{\partial t}. \tag{3.1}$$

Here H is the Hamiltonian, Ψ is the N particle time-dependent wave-function, and $\hbar$ is the Planck's constant divided by 2π.

In most cases time-dependent Schrödinger equation (TDSE Eq. 3.1) is not exactly solvable. This results in the necessity of approximate methods to solve the Schrödinger equation. Approximations are not usually sufficient for adequate analytic solutions. Computational methods provide us a very useful tool. Of course the problem should be solved in a continuous space, but numerically this is not possible. One should discretize the Schrödinger equation for a numerical study. In this chapter the method of discretization, an easier way to count the states and to find the matrix elements, and the algorithm of time development

for the solution of the time-dependent equation will be explained.

3.2 The Method

The method we propose begins with separating the Hamiltonian in two parts :

$$H = H_0 + H_1 \tag{3.2}$$

where H_0 is composed of terms including single particle parts of the Hamiltonian, and H_1 contains interaction between particles,i.e.,

$$H_0 = \sum_{i=1}^{N} h_i \tag{3.3}$$

and

$$H_1 = \sum_{i>j=1}^{N} V(x_i, x_j). \tag{3.4}$$

It is supposed that the equation

$$H_0 \psi_K(x) = E_K \psi_K(x) \tag{3.5}$$

and

$$h_i \phi_k(x) = \epsilon_k \phi_k(x) \tag{3.6}$$

are exactly solvable, with eigenstates $\phi_k(x)$, eigenvalues ϵ_k, and $E_K = \sum_{i=1}^{N} \epsilon_i$.

We will discuss our method in 1-dimensional case, although in general application to higher dimensions is always possible. For a general transport problem, the method we propose to solve the Schrödinger equation brings many simplifications and the solution is exact except the discretizations. Our model basically depends on solving the Schrödinger equation in a discretized spectrum of H_0, mainly discretizing the wavenumber spectrum. ·

Suppose that wavenumbers are discretized so that $1, 2, 3, \cdots$ denote the single particle quantum states in discrete spectrum of the non-interacting Hamiltonian H_0. Although in general, for a quantum transport problem, wavenumbers form a continuous spectra, we will use a discrete spectrum assuming that with small Δk

intervals we can expand any function with a negligible error. For example for a 1-dimensional problem it is assumed that wavenumbers, k's takes on values :

$$k = q\Delta k \tag{3.7}$$

with $q = \cdots, -2, -1, 0, 1, 2, \cdots$

Now the states are discrete, but as far as k can take on values from $-\infty$ to $+\infty$, again there are infinite number of single particle states. At this point one needs to put an upper bound for $|k|$, depending on the energy range of interest. For example for a resonant tunneling problem, if we are interested in only with the first resonance, then an upper energy which is less then the energy of the second resonance may be convenient. Clearly by using an upper bound, the number of single particle states becomes finite. In general, the new states now do not form a complete set of states. We can use these states as a basis to a good approximation if the contribution from remaining states is small.

Consider a quantum transport problem where the interaction H_1 is small compared to the energy of the incident particles and compared to the energy range which is being used. Under these assumptions expanding the solution of Eq. 3.1, it can be seen that expansion coefficients for the states that are not included in the basis is almost zero. In other words, error due to exclusion of the states from the basis is negligible.

When there is no interaction between particles the many particle wave-function and the total current for the system can be determined easily, by multiplying all the single particle states for a given N-particle state and anti-symmetrizing it using the Slater determinant. When the interaction exists the problem is more complicated. The following notation will be used in this chapter.

Ψ : many particle wave-function including spins

ϕ : single particle wave-function excluding spin

ψ : single particle wave-function including spin

ξ : spin part of the single particle wave-function

k : quantum state excluding the spin

s : spin value $+1(+)$ for spin up particle, $-1(-)$ for spin down particles.

Suppose a Fock basis for single particle wave-functions of the form

$$\psi_{k,s}(x) = \phi_k(x)\xi_s. \tag{3.8}$$

Here $\phi_k(x)$ represents the space part and ξ_s represents the spin part of the particle. s can take values of 1 and -1 only. By definition ξ_1 and ξ_{-1} form a complete set of states, i.e.,

$$\begin{aligned} &< \xi_1|\xi_{-1} >= 0 \\ &< \xi_1|\xi_1 >= 1 \qquad \text{and} \\ &< \xi_{-1}|\xi_{-1} >= 1 \end{aligned} \tag{3.9}$$

Also ϕ_k 's form a complete set of orthonormal basis for coordinate space, i.e.,:

$$< \phi_k|\phi_q >= \begin{cases} 1 & \text{if } k = q \\ 0 & \text{otherwise} \end{cases} \tag{3.10}$$

To find the many particle interacting solution we expand the solution at any time t , in terms of many particle non-interacting states. After discretizations, assuming that there are M different single particle states, the non-interacting basis for an N electron system will be of the form :

$$\frac{1}{\sqrt{(N!)}} \det \begin{bmatrix} \psi_{k_1}(x_1) & \psi_{k_1}(x_2) & & & & \psi_{k_1}(x_N) \\ \psi_{k_2}(x_1) & \psi_{k_2}(x_2) & & & & \psi_{k_2}(x_N) \\ & & & & & \\ & & & & & \\ \psi_{k_N}(x_1) & \psi_{k_N}(x_2) & \cdots & \cdots & \cdots & \psi_{k_N}(x_N) \end{bmatrix} \tag{3.11}$$

Consider a spin independent interaction potential, so that total spin will be conserved at all times. If for example, the incident state is composed of particles such that half of the spins are up and half are down, then total spin at time $t = 0$ is zero. This implies that total spin is always zero. This fact reduces the number of many particle states we should deal with. In fact for completeness we need

to include all the states, but because of the properties of the potential we can easily conclude that in any expansion of the wave-function corresponding to this incident state, the coefficient of such states are zero.

3.3 Representation

Next step when solving the problem should be to find an easy representation for the many particle states. We select a representation of the form

$$\Psi_{K,S} \rightarrow |k_1, k_2, \cdots, k_{\frac{N}{2}}; k_{(\frac{N}{2}+1)}, \cdots, k_N > . \tag{3.12}$$

Here $k_1, k_2, \cdots, k_{\frac{N}{2}}$ represents single particle states with spin part up and $k_{(\frac{N}{2}+1)}, \cdots, k_N$ represents states with spin part down. Rearranging the single particle states as spin up and spin down provides us convenience in manipulating the matrix elements. This is because of the Pauli exclusion principle. We know that no more than one fermion can exist in the same quantum state. Therefore the representation in Eq. 3.12 should be understood as a many particle state where particles occupy the single particle states $k_1, k_2, \cdots, k_{\frac{N}{2}}, k_{\frac{N}{2}+1}, \cdots, k_N$ and k_i 's are sorted in a way that first half are spin up all different, second part are spin down and all different.

To be more clear, consider two particles in single particle states k and q, k with spin up and q with spin down. Then corresponding two particle wave-function is of the form:

$$\Psi_{(k,+),(q,-)}(x_1, x_2) = \frac{1}{\sqrt{(2!)}}(\psi_{k,+}(x_1)\psi_{q,-}(x_2) - \psi_{q,-}(x_1)\psi_{k,+}(x_2)) \tag{3.13}$$

We represent this state by $|k; q>$.

And a four particle state composed of states $(k,+),(q,-),(r,+),(t,-)$ will be represented as:

$$|k, r; q, t> \tag{3.14}$$

This way of representing the many particle states brings us simplicity in counting the states. Since the particles are indistinguishable and the solution

is unique, we can bring a further restriction on the representation such that in a state

$$|k_1, k_2, \cdots, k_{\frac{N}{2}}; k_{(\frac{N}{2}+1)}, \cdots, k_N > \tag{3.15}$$

following inequalities should be satisfied.

$$k_1 < k_2 < \cdots < k_{\frac{N}{2}}$$

and

$$k_{(\frac{N}{2}+1)} < \cdots < k_N.$$

This means, first of all we enumerate single particle states as $1, 2, \cdots, M$ and now k_i 's may take only these values.

Assume we have M different single particle states (of course M is infinity for a continuous problem but we only take into account a discretized base). Call these states $1, 2, \cdots, M$. Then a six particle state composed of three electrons with spin up in states 2, 5, 6 and three electrons with spin down in states 4, 5, 8 is represented by:

$$|2, 5, 6; 4, 5, 8 >$$

but not

$$|5, 2, 6; 4, 8, 5 >$$

or

$$|4, 5, 8; 2, 5, 6 > .$$

The advantage of using this representation will be more clear when finding matrix elements between states.

Then next step should be to find the matrix elements corresponding to a two-particle-interaction. The interaction in general can be written as:

$$H_1 = V(x_1, x_2, \cdots, x_N) = u(x_1, x_2) + u(x_1, x_3) + \cdots + u(x_{N-1}, x_N). \tag{3.16}$$

An interaction of type $u(x_i, x_j) = u(x_i - x_j)$, which is the usual case, will be assumed.

We will calculate :

$$< k_1, k_2, \cdots, k_{\frac{N}{2}}; k_{(\frac{N}{2}+1)}, \cdots, k_N | V(x_1, x_2, \cdots, x_N) | q_1, q_2, \cdots, q_{\frac{N}{2}}; q_{(\frac{N}{2}+1)}, \cdots, q_N > . \tag{3.17}$$

Wave-function on the left is :

$$\frac{1}{\sqrt{(N!)}} \det \begin{bmatrix} \psi_{k_1}(x_1) & \psi_{k_1}(x_2) & & & & \psi_{k_1}(x_N) \\ \psi_{k_2}(x_1) & \psi_{k_2}(x_2) & & \cdots & & \psi_{k_2}(x_N) \\ & & & & & \\ \psi_{k_N}(x_1) & \psi_{k_N}(x_2) & \cdots & \cdots & \cdots & \psi_{k_N}(x_N) \end{bmatrix} \tag{3.18}$$

and wave-function on the right is:

$$\frac{1}{\sqrt{(N!)}} \det \begin{bmatrix} \psi_{q_1}(x_1) & \psi_{q_1}(x_2) & & & & \psi_{q_1}(x_N) \\ \psi_{q_2}(x_1) & \psi_{q_2}(x_2) & & & & \psi_{q_2}(x_N) \\ & & & & & \\ \psi_{q_N}(x_1) & \psi_{q_N}(x_2) & \cdots & \cdots & \cdots & \psi_{q_N}(x_N) \end{bmatrix} . \tag{3.19}$$

Ignoring the $\frac{1}{\sqrt{(N!)}}$ factor, the product of terms in the diagonal may be written as:

$$\psi^*_{k_1}(x_1)\psi^*_{k_2}(x_2)\cdots\psi^*_{k_N}(x_N)$$

and

$$\psi_{q_1}(x_1)\psi_{q_2}(x_2)\cdots\psi_{q_N}(x_N).$$

In each of the determinants, there are a total of $N!$ such products, each coming in with a plus or minus sign, depending on the number of permutations in the coordinate variable with respect to the term given above.

We are trying to find the matrix elements, so we are trying to evaluate (only considering the first term in V):

$$\int_{-\infty}^{\infty} dx^N \psi^*_{k_1}(x_1)\psi^*_{k_2}(x_2)\cdots\psi^*_{k_N}(x_N)u(x_1, x_2)\psi_{q_1}(x_1)\psi_{q_2}(x_2)\cdots\psi_{q_N}(x_N). \tag{3.20}$$

Because of the orthogonality of single particle wave-functions, we can clearly write this integral as :

$$\delta_{k_3 q_3} \cdots \delta_{k_N q_N} \int_{-\infty}^{\infty} dx_1 dx_2 \psi^*_{k_1}(x_1)\psi^*_{k_2}(x_2)u(x_1,x_2)\psi_{q_1}(x_1)\psi_{q_2}(x_2). \qquad (3.21)$$

It is obvious that this integral does not vanish only if single particle states for $i > 2$ in both wave-functions including the spin state are same. Only using the first terms of both wave-functions and first term in the potential, we can conclude that the matrix elements between two many-particle states is nonzero only if at least $N-2$ of the single particle states of both states are same.

At this point for the rest of the calculations we need to redefine the wave-function on the right in Eq. 3.19. What we know is that for a non-vanishing term in the matrix element at most two of the single-particle states should be different. Then for states differing three states from each other we do not need to calculate the matrix element but we simply put zero.

Assume now that the right hand side (RHS) wave-function which is formed of q's that differ from the left hand side (LHS) wave-function by most two single particle states. Then rearrange the terms in the determinant in the RHS wave-function in such a way that same single particle quantum states in the RHS wave-function appears in the same row as in the LHS wave-function. Due to properties of determinants, interchanging two rows results in a sign change. So the new RHS wave-function and the older one differ only by a sign depending on the number of interchanges to rearrange the rows. If we have done an even number of interchanges the two wave-function are exactly the same but if the number of interchanges is odd the newer one is -1 times the older one.

As an example, suppose a six particle wave-function on the left hand side of the form $< 2,5,6;4,5,8|$. A term on the RHS contributing to the matrix element may be $|2,4,5;3,4,8>$. We choose new q's so that the new RHS is $|2,5,4;4,3,8>$.

Let us return to the method. Now consider another term in the new wave-function on the right :

$$\psi^*_{k_2}(x_1)\psi^*_{k_3}(x_2).....\psi^*_{k_N}(x_{N-1})\psi^*_{k_1}(x_N) \qquad (3.22)$$

and corresponding integral is :

$$\delta_{k_4 q_3}.....\delta_{k_1 q_N} \int_{-\infty}^{\infty} dx_1 dx_2 \psi^*_{k_2}(x_1)\psi^*_{k_3}(x_2)u(x_1,x_2)\psi_{q_1}(x_1)\psi_{q_2}(x_2). \tag{3.23}$$

But in choosing k's and q's it is said that first half of both are spin up states and second half are spin down states. So at least $\delta_{k_1 q_N} = 0$ since they have different spin states. Then the whole integral is zero. This is a simplification n in evaluating the integrals coming from the choice of representation.

For simplicity in notation let us denote the integral

$$\prod_{k,q} \delta_{kq} \int_{-\infty}^{\infty} dx_r dx_s \psi^*_{k_i}(x_r)\psi^*_{k_j}(x_s)u(x_r,x_s)\psi_{q_l}(x_r)\psi_{q_m}(x_s) \tag{3.24}$$

by

$$V(k_i, k_j; q_l, q_m).$$

Using the previous results on integrals and using the properties of the determinant we get :

$$((N-2)!)\sum_{i=1}^{\frac{N}{2}}\sum_{j=1}^{\frac{N}{2}} V(k_i, k_{j+\frac{N}{2}}; q_i, q_{j+\frac{N}{2}}) \tag{3.25}$$

corresponding not to the whole matrix element but only to the first term in the potential.

Now let us consider the other terms in the potential. Take $u(x_i, x_j)$. The calculations need not be repeated in order to find the part of the matrix element that corresponds to this term in the integral. Assume that the 1^{st} and i^{th} column are interchanged and 2^{nd} and j^{th} column in the wave-function on the left. Also do the same interchanges in the wave-function on the right. For the first changes we will get + or − times the same wave-function depending on the number of interchange and for the RHS again we will get + or − times the same RHS. Important thing is that same permutations are performed on both wave-function so that they will have same sign as a multiplier. But the matrix element is found from the product of these two wave-functions. It can be concluded that the total multiplier due to the interchanges will be one.

The only difference is that the integrals in definition of $V(k_i, k_j; q_l, q_m)$ will be carried out with respect to x_i and x_j but in the new form of the wave-functions; it is same as integral with respect to x_1 and x_2 using the previous wave-functions. The result is then the same, again due to the indistinguishability of the particles.

There are $\frac{N(N-1)}{2}$ terms in the potential of the form $u(x_1, x_2)$. As a result the matrix element between these two states is

$$((N-2)!)\frac{N(N-1)}{2}\sum_{i=1}^{\frac{N}{2}}\sum_{j=1}^{\frac{N}{2}} V(k_i, k_{j+\frac{N}{2}}; q_i, q_{j+\frac{N}{2}}). \tag{3.26}$$

Remember that in the beginning of the calculations, we ignored the multipliers $\frac{1}{\sqrt{(N!)}}$ of the wave-functions. Then the final result is

$$\frac{1}{2}\sum_{i=1}^{\frac{N}{2}}\sum_{j=1}^{\frac{N}{2}} V(k_i, k_{j+\frac{N}{2}}; q_i, q_{j+\frac{N}{2}}) \tag{3.27}$$

As can be seen from this summation we need only to calculate $\frac{N^2}{4}$ integrals. If we did not use this representation and just expand the determinant we should calculate $(N!)^2$ integrals which is much larger than $\frac{N^2}{4}$.

3.4 Algorithm

Our procedure for solving the time-dependent Schrödinger equation depends on discretizing the time-steps. Consider an Hamiltonian of the form

$$H = H_0 + \sum_{i>j=1}^{N-1} u(x_i, x_j). \tag{3.28}$$

Here as mentioned earlier we assume that H_0 part can be solved exactly,

$$H_0 = \sum_i [-\frac{\hbar^2}{2m}\nabla_i^2 + v(x_i)] \tag{3.29}$$

and

$$u(x_i, x_j) = u(x_i - x_j). \tag{3.30}$$

We know that time independent solutions of the single particle Schrödinger equation form a complete set of states. Many particle solution follows from proper anti-symmetrization of products of single particle solutions. At this point the spectrum of the Hamiltonian H_0 will be discretized as described before in this chapter.

The many particle Schrödinger equation is then

$$(H_0 + \sum_{i>j=1} u(x_i, x_j))\Psi(x_1, x_2, x_3, \cdots, t) = i\hbar \frac{\partial \Psi(x_1, x_2, x_3, \cdots, t)}{\partial t}. \tag{3.31}$$

Then at any time t the solution may be written in the form

$$\Psi = \sum_q A_q(t)\Phi_q(x_1, x_2, \cdots) \tag{3.32}$$

where Φ 's stand for complete set of many particle solutions. Also

$$H_0\Phi_q = E_q\Phi_q \tag{3.33}$$

is known. Substituting this form of solution in the Eq. 3.31, we get

$$H_0 \sum_q A_q\Phi_q + \sum_{i>j=1}^{N} u(x_i, x_j) \sum_q A_q\Phi_q = i\hbar \sum_q \Phi_q \frac{\partial A_q}{\partial t}. \tag{3.34}$$

Now by using the substitution $A_q(t) = e^{-it\frac{E_q}{\hbar}}F_q(t)$ we switch from the Schrödinger representation to the interaction representation. We now have the equation

$$\sum_q exp(-it\frac{E_q}{\hbar})F_q(t)E_q\Phi_q + \sum_{i>j=1}^{N} u(x_i, x_j) \sum exp(-it\frac{E_q}{\hbar})F_q(t)\Phi_q \tag{3.35}$$

$$= i\hbar \sum \Phi_q(\frac{-iE_q}{\hbar}exp(-it\frac{E_q}{\hbar})F_q(t) + exp(-it\frac{E_q}{\hbar})\frac{\partial F_q}{\partial t}).$$

After simplifying this equation we get

$$\sum_{i>j=1}^{N} u(x_i, x_j) \sum_q e^{-it\frac{E_q}{\hbar}}F_q(t)\Phi_q = i\hbar \sum \Phi_q e^{-it\frac{E_q}{\hbar}} \frac{\partial F_q}{\partial t}. \tag{3.36}$$

Multiplying this equation by ϕ_k^* and integrating over all x_i 's yields :

$$\sum_q V_{k,q} e^{-it\frac{E_q}{\hbar}} F_q(t) = i\hbar e^{-it\frac{E_k}{\hbar}} \frac{\partial F_k}{\partial t}. \tag{3.37}$$

We assume that at time $t = 0$ the interaction is zero, and then we adiabatically increase the potential to its final value. An adiabatic time-dependence for the interaction given by $\lambda(t)$ is introduced, so that interaction potential is given by:

$$u(x_i, x_j)\lambda(t). \tag{3.38}$$

There is still a problem in solving this equation. One method to solve this equation would be using Monte Carlo techniques such that we could write time-dependent solution of the form:

$$F_q(t) = (e^{-i\frac{t-t_0}{M}\frac{V}{\hbar}})^M F_q(t_0) \tag{3.39}$$

as M goes to infinity.

Here V represents the total interaction but not a constant, and it is not diagonal in this representation. So to find the time-dependence of the coefficients we should find another method. Another approach may be discretizing the time derivative in Eq. 3.37 . Experience in solving the Schrödinger Equation numerically has shown that to obtain an accurate wave-function, the algorithm must preserve the norm, and the time reversal symmetry. One method may be the obvious one

$$\frac{\partial F_q(t)}{\partial t} = lim_{\Delta t \to 0} \frac{F_q(t + \Delta t) - F_q(t)}{\Delta t}. \tag{3.40}$$

It is easy to see that norm is conserved to order (Δt) but the time reversal symmetry is broken i.e., one will not obtain $F(t)$ back from $F(t + \Delta t)$ by the same process. Instead we may try

$$\frac{\partial F_q(t)}{\partial t} = lim_{2\Delta t \to 0} \frac{F_q(t + \Delta t) - F_q(t - \Delta t)}{2\Delta t}. \tag{3.41}$$

By inserting this into equation 3.37 and after a simple algebra we get the result

$$F_q(t + \Delta t) = F_q(t - \Delta t) - \frac{2i\Delta t}{\hbar} \lambda(t) \sum_k V_{q,k} e^{-\frac{i(E_k - E_q)t}{\hbar}} F_k(t). \tag{3.42}$$

Knowing the wave-function at time $t = 0$, the wave-function at all times can be found. Here it can be shown that time reversal symmetry is conserved, and the norm is conserved in the order of (Δt).

3.5 Test of the method (single barrier)

We will test our algorithm and discretization procedure using a 1-dimensional quantum system with a single delta function potential located at $x = 0$. This is a good test of the method, because first of all the exact solution is known, so that we can compare the results and see if the discretizations cause a big error or not, secondly in the next chapter we will apply the method to a 1-dimensional double barrier system with electron-electron interactions of similar form.

Consider that the Hamiltonian whose solutions are known is the free particle Hamiltonian in this test, and the interaction which will be supposed to have an adiabatic time-dependence is the barrier located at $x = 0$. The geometry corresponding to this simple test is shown in Fig. 3.1.

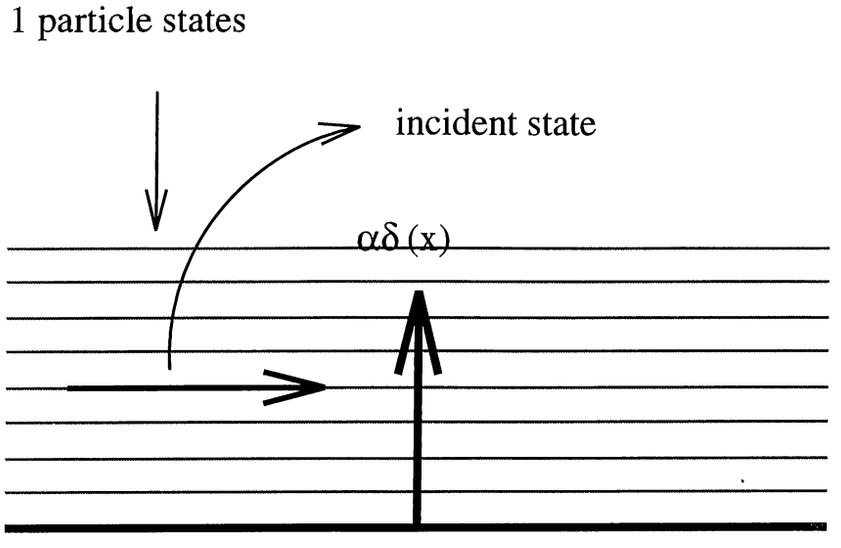

Figure 3.1: Energy profile of the single barrier structure.
This delta potential corresponds to electron-electron interaction in the model, in the next chapter

Schrödinger equation we need to solve is :

$$[H_0 + \alpha\delta(x)]\phi(x,t) = i\hbar\frac{\partial\phi(x,t)}{\partial t} \tag{3.43}$$

where

$$H_0 = \frac{-\hbar^2}{2m^*}\frac{\partial^2}{\partial x^2}. \tag{3.44}$$

Indeed this is an exactly solvable and separable problem. Separating $\phi(x,t)$ as $\varphi(x)T(t)$ we can write the solution for a particle incident from right with energy $E = \frac{\hbar^2k^2}{2m^*}$ as :

$$\varphi(x) = \begin{cases} e^{ikx} + re^{-ikx} & \text{if x} < 0 \\ te^{ikx} & \text{if x} > 0 \end{cases} \tag{3.45}$$

and

$$T(t) = e^{-\frac{iEt}{\hbar}} \tag{3.46}$$

with $r = u/(2ik - u)$ and $t = 2ik/(2ik - u)$. Here u is $2m^*\alpha/(\hbar^2)$.

Now let us apply our methodology and see if the results fit the exact results given above. As explained we assume that the Schrödinger equation with zero interaction is exactly solvable. If $\alpha = 0$ we should solve time independent Schrödinger equation :

$$H_0\varphi(x) = E\varphi(x) \tag{3.47}$$

and the solutions can be written as :

$$\varphi_k(x) = \frac{1}{\sqrt{(2\pi)}}e^{ikx} \tag{3.48}$$

with energy $E = \frac{\hbar^2k^2}{2m^*}$. Here k values are continuous. As explained in the previous sections, let us discretize these values such that $k = n\Delta k$ with n being an integer, and let us put an upper bound for $|k|$, say $|k_{max}| = m\Delta k$. Let us denote $\varphi_{k=m\Delta k}(x)$ by φ_m.

Assume an adiabatic time-dependence for the potential as

$$\lambda(t) = \begin{cases} 0 & \text{if } t < 0 \\ 0.5(cos(t+\pi)+1) & \text{if } 0 < t < t_0 \\ 1 & \text{if } t > t_0 \end{cases} \tag{3.49}$$

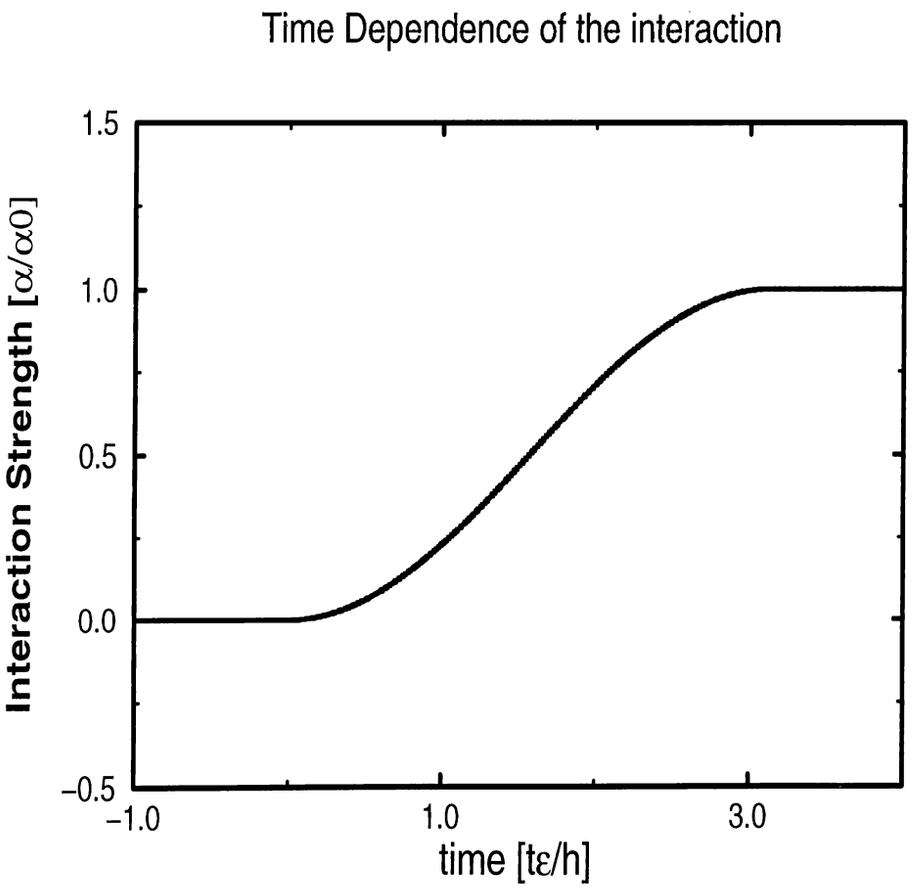

Figure 3.2: Time-dependence of the interaction strength.

which is drawn in figure 3.2.

Then we should solve the equation :

$$[H_0 + \alpha\delta(x)\lambda(t)]\phi(x,t) = i\hbar\frac{\partial\phi(x,t)}{\partial t} \tag{3.50}$$

We suppose that for a particle incident from right with energy E_0 the solution can be written as :

$$\phi(x,t) = \sum_{j=-m}^{m} A_j(t)\varphi_j(x). \tag{3.51}$$

Inserting this into Eq. 3.50, multiplying this equation by $\varphi_n^*(x)$ and integrating over x, because of orthogonality we get :

$$A_n(t)E_n + \frac{\alpha\lambda(t)}{2\pi}\sum_{j=-m}^{m} A_j(t) = i\hbar\frac{\partial A_n(t)}{\partial t} \tag{3.52}$$

After defining $F_n(t)$ as explained before, we are left with :

$$F_n(t+\Delta t) = F_n(t-\Delta t) - i\frac{\alpha\lambda(t)}{2\pi}\frac{2\Delta t}{\hbar}\sum_{j=-m}^{m} F_j(t)e^{\frac{-i(E_j-E_n)t}{\hbar}} \tag{3.53}$$

We assume that at time $t = -\Delta t$ and $t = 0$ wave-function is given by the initial state.

Then we can find numerically the wave-function at any time.

For $\Delta k = 0.1$, $\Delta t = \pi/5000.0$, $m = 325$, we get the results shown in the next section.

3.5.1 Results

In all the results that will be shown here and that was shown in Fig. 3.2 energy is scaled with $\epsilon = \hbar^2/(2md^2)$ with d chosen arbitrarily for the time being. Then time is scaled with $t_0 = \hbar/\epsilon$.

In this section the results for this simple geometry will be demonstrated. In Fig. 3.3 square magnitude of the wave-function throughout the structure for time, corresponding to a time greater than the time value where the interaction is fully turned on, is drawn for an interaction $\alpha = 10$. In the same figure, exact result is also drawn. In Fig. 3.4 same quantities for an interaction strength $\alpha = 8$ is drawn. From these two figures one can see that the results from the method and the exact results are almost same. Solid lines are the results of the method and dashed lines are exact results.

To give an idea about how the wave-function evolves in time for the given time-dependence of the interaction, time-dependence of the square magnitude of the wave-function is drawn in Fig. 3.5.

The square magnitudes of the expansion coefficients are drawn, in Fig. 3.6 for a time $t > t_0$. This last figure has special importance for our purposes. As said earlier, interaction in this test model is of the similar type as the one that will

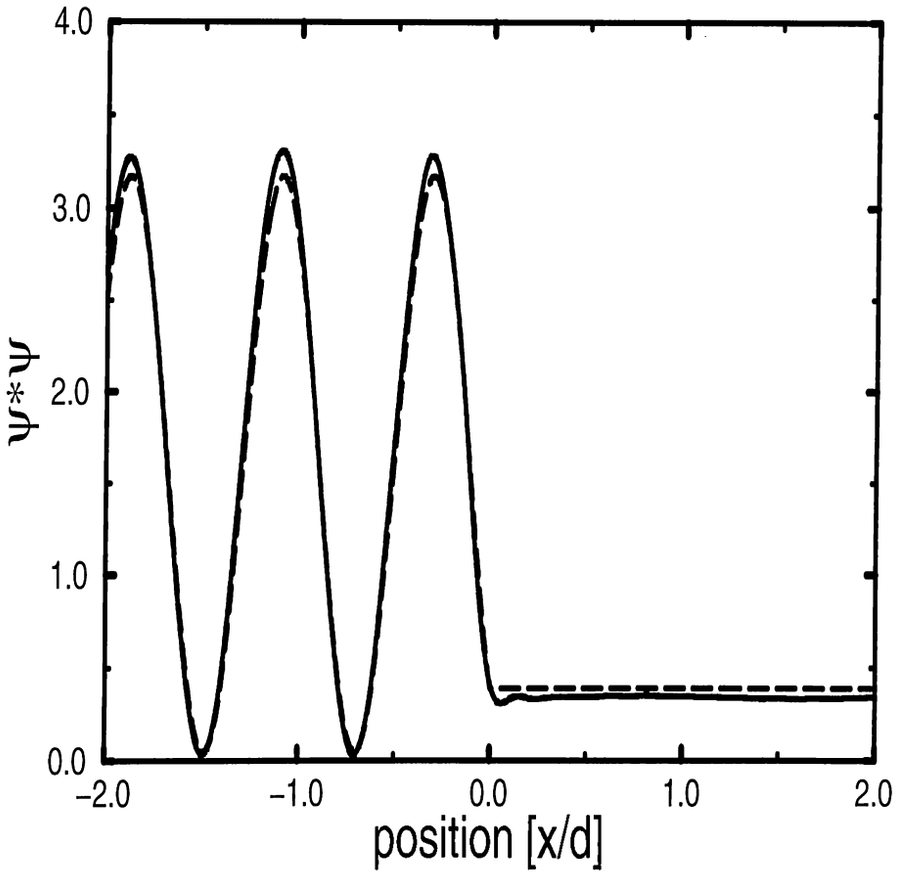

Figure 3.3: Square magnitude of the wave-function versus position, for $\alpha = 10$. Solid line is the result of our method. Dashed line is the exact result.

be used as electron-electron interaction in the next chapter. From the Fig. 3.6, it can be concluded that for an interaction of type delta function, the coefficients of states of energy far from the energy of the incident wave is almost zero. In the figure $k = 4$ and $k = -4$ have the maximum amplitudes, where both correspond to the energy of the incident wave. Then we can use as a base, a set of states whose energy is about the energy of the incident wave. Of course for the model in the next chapter, this result is not enough, but at least gives the idea about the minimum number of states necessary to obtain an accurate result.

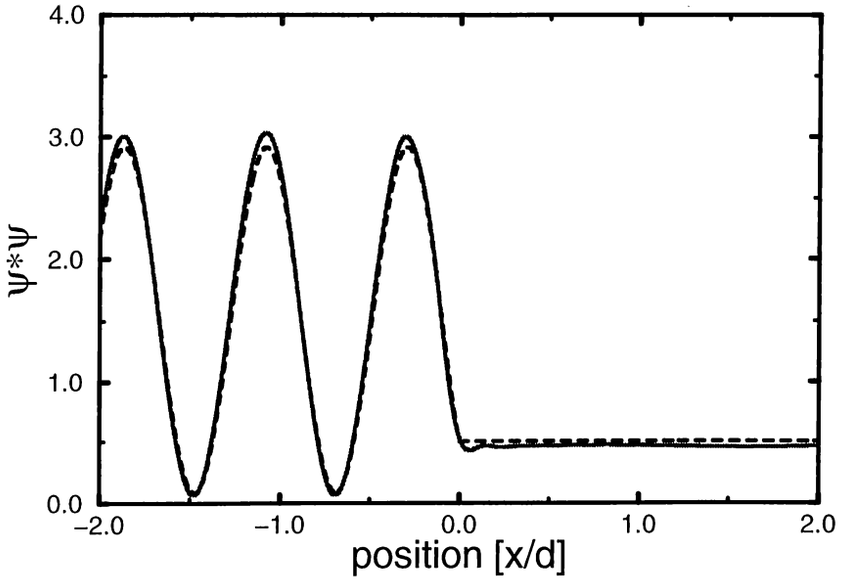

Figure 3.4: Square magnitude of the wave-function versus position, for $\alpha = 8$. Solid line is the result of our method. Dashed line is the exact result.

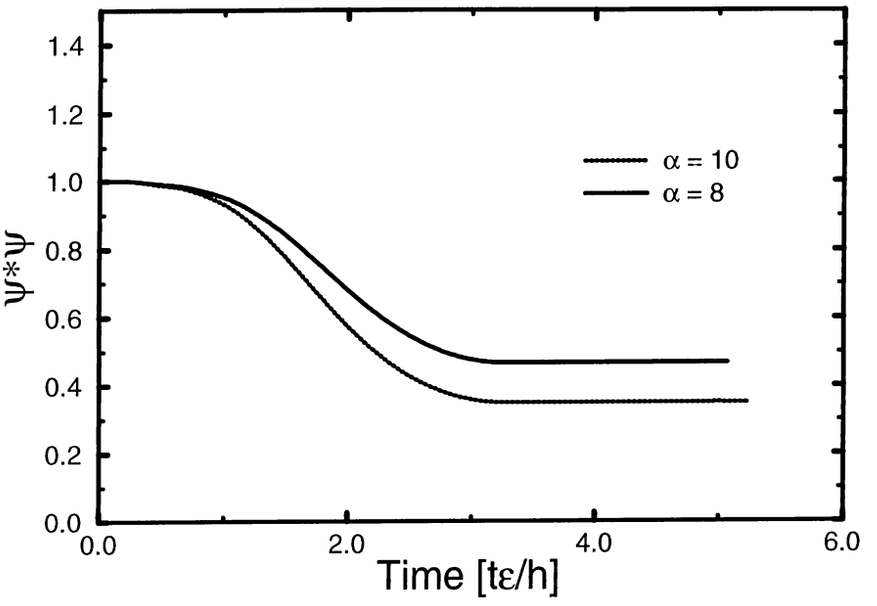

Figure 3.5: Time evolution of the square magnitude of the wave-function. It is calculated at an arbitrary location $x > 0$. The results are for $\alpha = 10$ and $\alpha = 8$.

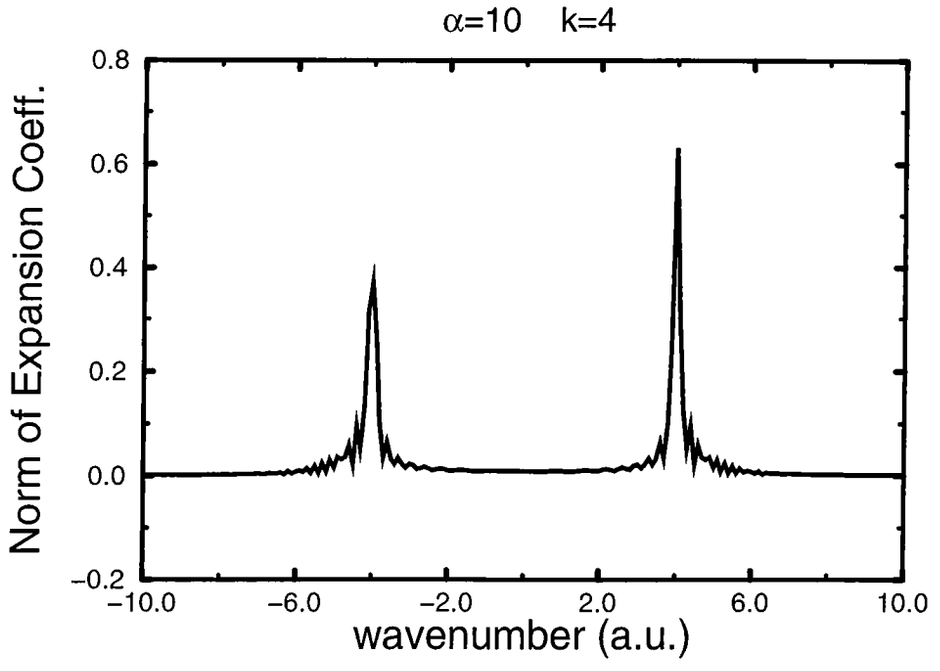

Figure 3.6: Square magnitude of the expansion coefficients.
Both axes are drawn in arbitrary units. The states with equal energy as the incident state have the greatest magnitudes. As the energy difference with the incident state becomes large, expansion coefficients decreases exponentially.

Chapter 4

DOUBLE BARRIER STRUCTURE

4.1 Introduction

After the work of Tsu, Esaki, and Chang [1–3] there has been a great deal of interest in resonant tunneling diodes (RTD's), where a double barrier (DB) structure is one of the most promising example. Tsu, Esaki and Chang has demonstrated [1] that these structures exhibits negative differential resistance.

Although the current-voltage ($I - V$) characteristics of resonant tunneling (RT) structures are well understood by direct quantum mechanical calculation of tunneling transmission through the structure, there are still scientist working on this area, may be due to the rapid developments in the technology of semiconductor devices. With the advance of the fabrication techniques, it is now possible to fabricate devices with very small dimensions, and many technological applications are possible. For example, these structures may be used as memory storage units or circuit elements, etc.

On the other hand, the problem of the double barrier resonant tunneling structure contains interesting physics: Tunneling is a manifestation of quantum physics, transport occurs in classically forbidden region. Also, DBRT structures exhibit a bistable behavior and hysteresis in the $I - V$ characteristics, which

are signatures of non-linear phenomena, and is challenging to study within the context of the linear quantum mechanical theory.

DBRT structures with dimensions smaller than electron phase coherence length where the transport is fully ballistic, can be routinely produced. Quantum mechanical analysis of these devices becomes more important since in this regime the transport properties of the devices can be determined only quantum mechanically. Fabricating smaller devices makes it possible that the first quasi-bound energy of the well is high enough to restrict the device work in the energy range of first quasi-bound energy, which is the energy of the first resonance for a DBRT structure.

4.2 A simple model

We simulate the potential energy of the double barrier structure simply by two symmetric delta functions located at $x = -d$ and $x = d$, i.e., the potential energy is given by :

$$V(x) = \begin{cases} \alpha[\delta(x-d) + \delta(x+d)] & \\ 0 & \text{otherwise} \end{cases} \tag{4.1}$$

Here α is the height of the barriers. For simplicity we simulated rectangular barriers with delta function barriers which is a limiting case of rectangular barriers.

Apart from the potential function of the barriers, an electron in the structure will feel the potential produced by other electrons. An electron-electron interaction in the form

$$V(x_i, x_j) = \begin{cases} \beta\delta(x_i - x_j) & \text{if} - d < x_i < d \\ 0 & \text{otherwise} \end{cases} \tag{4.2}$$

which provides considerable simplification with respect to more realistic potentials. Here β is the strength of the interaction.

The simplification of the inter-particle potential may be justified by the argument that this interaction is dominant in the region between the barriers,

where there is considerable charge build-up. Throughout the whole structure, except in the space between barriers, because of the screening effect of electrons (low density of electrons in these parts), electrons will not feel each other very strongly, but between the barriers, if the distance between the barriers is small, there will be a large confinement potential which corresponds to the quasi-bound energy of the well, so that there is a great charge accumulation between the barriers with strong inter-particle interaction. Note that the screening length of the electrons is given by

$$L_s = \frac{2}{\sqrt{a_B d}} \tag{4.3}$$

with a_B being the Bohr radius given by

$$a_B = \frac{4\pi\epsilon\hbar^2}{m^* e^2}. \tag{4.4}$$

For example for GaAs $m^* = 0.07m_e$ (mass of electron), and $\epsilon = 1.26$, so that a_B is about $10nm$ and screening length is about $5nm$. This provides some justification for the argument above.

Furthermore, it should be stated that our main interest in the following calculations is to study the appearance of bistability in resonant tunneling structures, and therefore we have made simplifications in the model to allow us to concentrate on this point.

Conventional model for a double barrier resonant tunneling structure is shown in figure 4.1.

Under an applied bias V, the conduction band minimum of the device throughout the space is drawn. Exact result for the conduction band minimum can be found by solving the Schrödinger equation involving the bias. Numerically this model is solvable, but is not convenient or necessary for our purposes. In this model charge accumulation is not only in the region between the barriers but also there exists charge accumulation at the left side of left barrier, which although may be a significant effect for a real device, is not relevant to our study of bistability. On the other hand, when the electron-electron interaction is zero, we would like to solve the Schrödinger equation exactly, which is not the case in this model. So we propose a simpler model, which does not cause charge

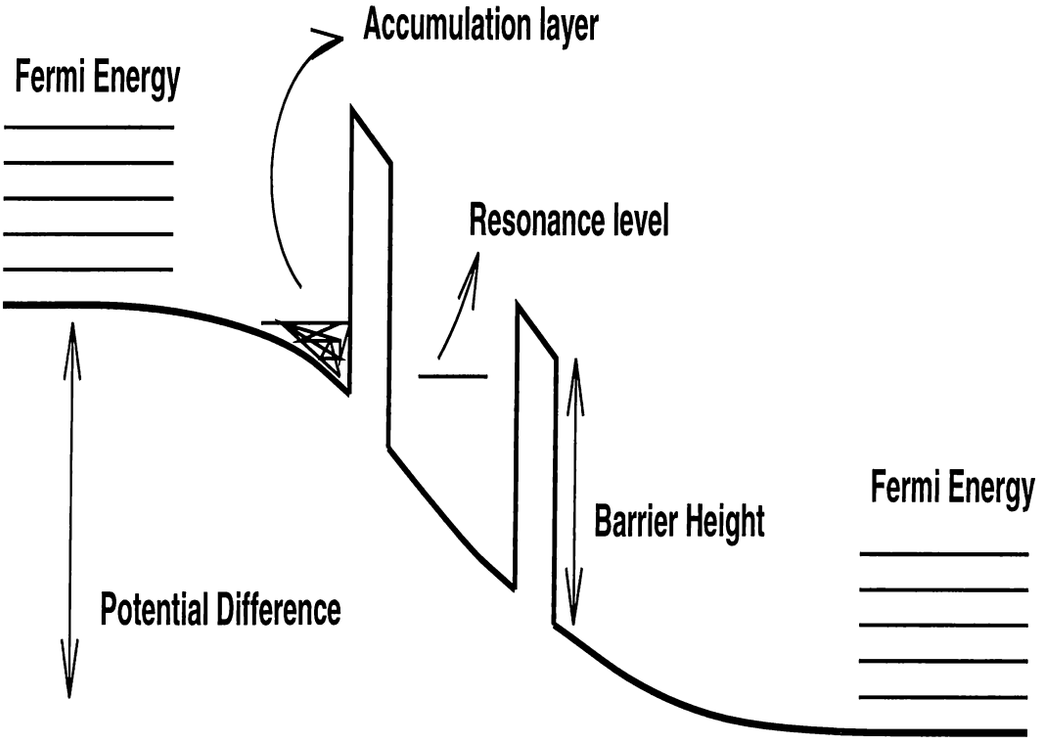

Figure 4.1: The conventional model for the energy profile of the double barrier structure.

accumulation except between barriers and which can be solved exactly when the electron-electron interaction is not present.

The model picture is shown in Fig. 4.2. Here $1, 2, \cdots, 8$ represents the single particle states. Reservoir is simulated by region I, at the left boundary, so that it can emit particles of total energy greater than V (the potential difference between right and left reservoirs). If it is assumed that the potential profile in region 1 is smooth enough, then particles incident from right with total energy below eV are reflected with a reflection coefficient r, nearly equal for the range, whose magnitude is unity. So it brings restriction to wave-function such that particles incident from right whose kinetic energy is below the potential difference do not carry current.

When a smoothness is assumed in region I, single particle solutions may be found. For our purposes, the important part of the problem is how the current

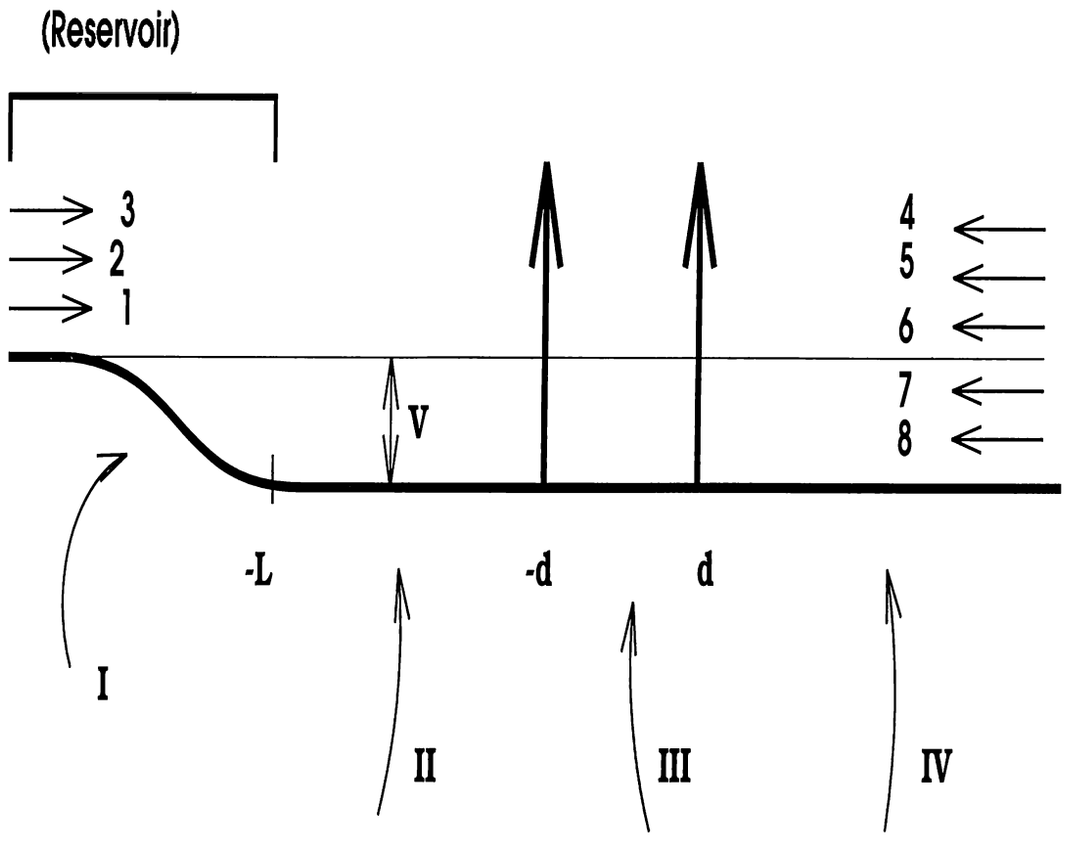

Figure 4.2: A simple model for double barrier resonant tunneling structures.

behaves under an applied bias. The transmission coefficient T is drawn in Fig. 4.3, which is nearly same as the results of the conventional model for double barrier resonant tunneling structures [41] shown in Fig. 4.3.

When calculating the transmission probabilities of the electrons, i.e., when solving the Schrödinger equation, we will assume a fully coherent transport, that is, an electron is transmitted from the left reservoir to the right reservoir in a single quantum mechanical process, whose probability can be calculated from the Schrödinger equation. This is true if the average time an electron spends in resonant state is much less than the scattering time T_Φ. On the other hand, if this is not the case, a significant fraction of the current is due to the sequential tunneling, where an electron first tunnels through the left barrier to the well, looses its phase information, then tunnels through the other barrier. It was

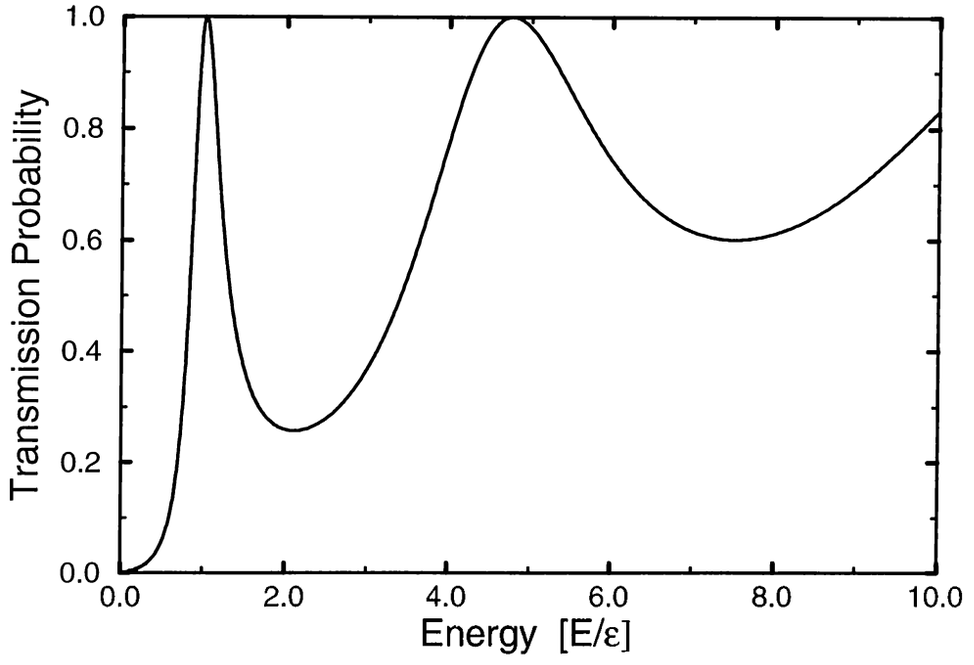

Figure 4.3: Transmission probability versus energy.
This transmission probability is obtained by using the simple model for the double barier resonant tunneling structure.

shown [42] that phase breaking process have little effect on the resonant tunneling current.

4.3 Bistability

The most general time independent Schrödinger equation for an n-particle system is:

$$[\sum_i(-\frac{\hbar^2\nabla^2}{2m}) + V(x_1, x_2, \cdots, x_n)]\psi(x_1, x_2, \cdots, x_n) = E\psi(x_1, x_2, \cdots, x_n). \quad (4.5)$$

Here E is the energy of the system and x_i refers to spatial and spin coordinate of the i^{th} particle. Mathematically, this is a linear equation. As known from basic linear algebra concepts, a linear equation may have only one solution (uniqueness of the solution in quantum mechanics) provided that boundary conditions are uniquely defined.

Whatever the potential function V is, ψ is uniquely determined. In short for a given energy E and given set of boundary conditions, there is only one solution ψ that satisfies the time independent Schrödinger equation 4.5. Obviously all the physical quantities, such as current, charge build-up etc. are expectation values of the corresponding quantum mechanical operator with respect to ψ. But experimentally it was shown that current-voltage, transmission-voltage, conductivity-voltage etc. exhibit a bistable behavior and a hysteresis, which seems to contradict with this basic principle of quantum mechanics i.e., uniqueness of the solution.

There are several explanations of the hysteresis loop for a double barrier resonant tunneling structure. First it should be mentioned that there exists a region called *negative differential resistance* (NDR), where current throughout the structure decreases as the applied bias voltage increases. This is one of the fundamental properties of resonant tunneling structures. Bistability is observed in this region. This bistability can be interpreted as an intrinsic feature arising from electrostatic effects due to the build-up of negative space-charge in the quantum well between the two barriers. It may be noted that there is at least a qualitative similarity between this bistable behavior and hysteresis loop, and the bistability and hysteresis that is seen in phase transitions.

It is clear that working with mean-field approaches, bistability can be obtained since in mean-field approaches one has to solve a nonlinear set of equations which may readily yield multi-stable solutions. Using a linear approach, such as the Schrödinger equation, one should not expect to see the effect but may observe indications of the bistability. Analogy with phase transitions would indicate that the solution is unique in this approach but there may exist unstable solutions which decay to a stable solution [43] or oscillate in time. In the next sections it will be shown that in the NDR region, depending on how the interaction is turned on, there are unstable solutions corresponding to bistable solutions in the experiments which oscillate in time.

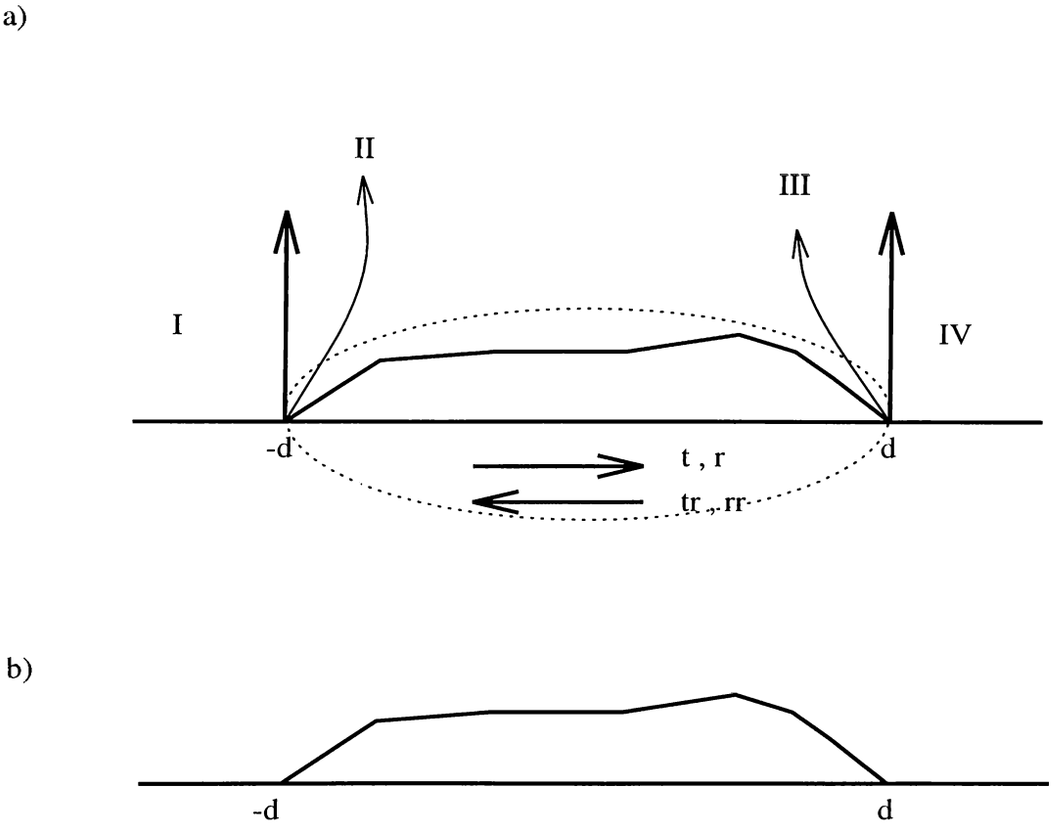

Figure 4.4: Energy profile of the double barrier structure.
a) Energy profile of the double barrier resonant tunneling structure with potential energy between the barriers arbitrarily drawn. This potential corresponds to total interaction given by the Hartree-Fock equations. b) Self-consistent potential between the barriers (arbitrarily drawn).

4.4 Mean-Field solution

In the time independent Schrödinger equation picture, the equation to be solved is Eq. 4.5. There is no straightforward method to solve the equation directly numerically, the difficulty arises due to the number of coordinate variables, which results in working in a N-dimensional complex space. We may consider an Hartree solution where the interaction is assumed to be separable to one body potentials. In other words the potential that is seen by an electron is assumed to consist of the other electrons' probabilities of being in the required place in the

space, times the strength of the interaction.

Hartree equations can be written as :

$$\frac{-\hbar^2\nabla_i^2}{2m}\phi_i(x_i) + U(x_i)\phi_i(x_i) + \sum_{j\neq i}\int dx_j V(x_i,x_j)\phi_j^*(x_j)\phi_j(x_j)\phi_i(x_i) = E_i\phi_i(x_i). \tag{4.6}$$

Here $U(x_i)$ is the potential energy function of the geometry and total energy of the system is given by $E = \sum_{particles} E_i$. For an interaction given by Eq. 4.2, this equation reduces to

$$\frac{-\hbar^2\nabla_i^2}{2m} + U(x_i) + \beta\sum_{j\neq i}\phi_j^*(x_i)\phi_j(x_i)\phi_i(x_i) = E_i\phi_i(x_i). \tag{4.7}$$

for the double barrier structure defined by Eq. 4.1.

Note that these set of equations does not satisfy Pauli exclusion principle. Instead, Hartree-Fock equations, which are modified versions of Hartree equations and which do satisfy the exclusion principle can be used, which read :

$$\frac{-\hbar^2\nabla_i^2}{2m}\phi_i(x_i) + U(x_i)\phi_i(x_i) + \sum_{spinvariable}\sum_{j\neq i}\int dx_j V(x_i,x_j)\phi_j^*(x_j)\phi_j(x_j)\phi_i(x_i)$$

$$-\sum_{j\neq i}\int dx_j V(x_i,x_j)\phi_i^*(x_j)\phi_j(x_j)\phi_i(x_i) = E_i\phi_i(x_i). \tag{4.8}$$

These equations may be obtained from an energy minimization procedure with the constraint of separability of the solutions.

If the interaction in Eq. 4.2 is taken, these equations reduce to the simple form

$$\frac{-\hbar^2\nabla_i^2}{2m} + U(x_i) + \beta\sum_{j}\phi_j^*(x_i)\phi_j(x_i)\phi_i(x_i) = E_i\phi_i(x_i). \tag{4.9}$$

These sets of equations can be solved self-consistently using an iterative algorithm. For the double barrier structure with given potential energy function in the previous section, the method to solve these equations is briefly explained, and the results are demonstrated.

Consider the Fig. 4.4. We define the regions I, II, III, IV in the figure and also the fifth region which is between the barriers, in the self-consistent potential

region. The corresponding wave-functions can be written as :

$$\phi(x) = \begin{cases} e^{ikx} + Re^{-ikx} & \text{in region I} \\ Ae^{ikx} + Be^{-ikx} & \text{in region II} \\ Ce^{ikx} + De^{-ikx} & \text{in region III} \\ Te^{ikx} & \text{in region IV} \end{cases} \tag{4.10}$$

In the region between barriers we define two wave-functions $\phi_{\rightarrow}$ and $\phi_{\leftarrow}$, which corresponds to a wave incident from left with $e^{ikx} + re^{-ikx}$ and transmitted as te^{ikx} and a wave incident from right with wave-function $e^{-ikx} + rre^{ikx}$ and transmitted as tre^{ikx} respectively, for the geometry shown in second figure in Fig. 4.4. Since these solutions can be determined trivially, the solution of the full problem reduces to solving a set of equations arising from boundary conditions. Boundary matching between regions I and II, and III and IV are obvious. The matching condition for the region II, III, and the well can be easily obtained by keeping in mind the way $\phi_{\rightarrow}$ and $\phi_{\leftarrow}$ are defined.

We can write the matching in this part as:

$$Ar + Dtr = B$$

$$C = At + Drr$$

and the wave-function between the barriers is $A\phi_{\rightarrow} + D\phi_{\leftarrow}$.

These equations can be solved provided that $\phi_{\rightarrow}$ and $\phi_{\leftarrow}$ are found. For a given interaction constant β, the solution can be found in several ways. Basically we take an initial guess for the wave-function, use this guess when finding the interaction potential and new wave-function, recursively continuing this process until convergence. There are various ways to determine the initial guess. The solution at zero interaction is known, so this solution can be used as an initial guess. When the solution at some applied bias V is found, this solution can be used as an initial guess for the applied bias $V + \Delta V$ or $V - \Delta V$. We can find the solution for the strength of the interaction greater than the actual value and use this solution as an initial guess for the wave-function we are seeking. The different ways to set the initial guess are tried.

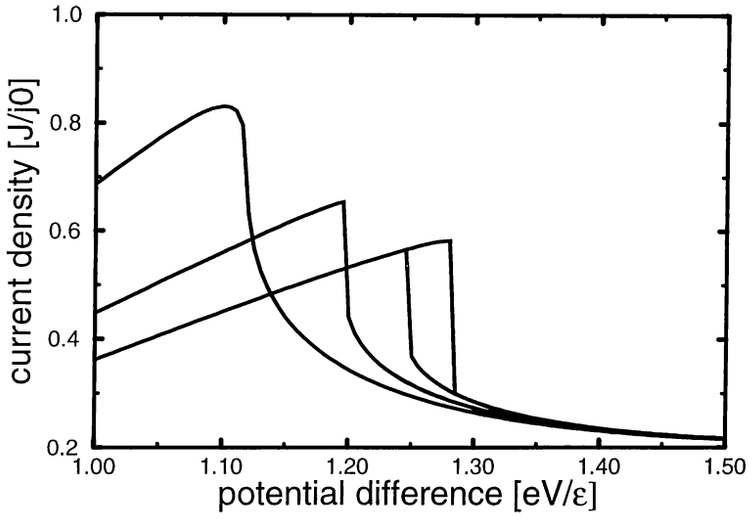

Figure 4.5: Mean Field Results
Current versus applied bias for four particles. The graphs are for interaction equals 0.001, 0.0015 and 0.0024 times ϵ from left to right respectively.

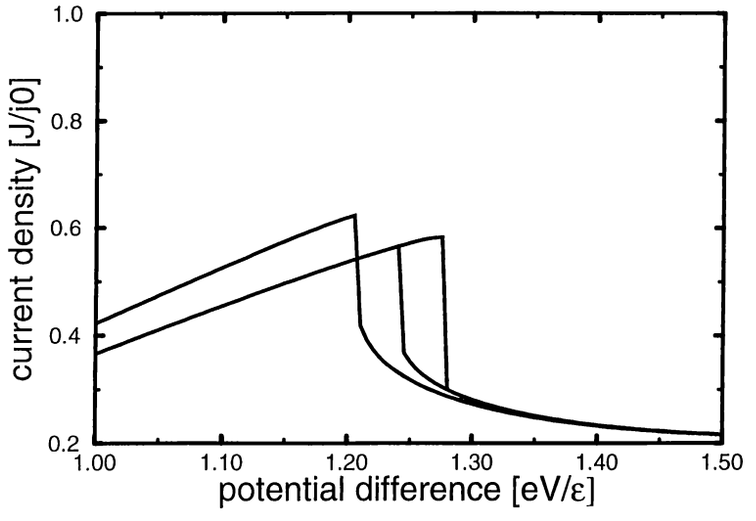

Figure 4.6: Current versus applied bias for eight particles.
The graphs are for interaction strength equals 0.0015 and 0.0024 times ϵ from left to right respectively.

4.4.1 Results

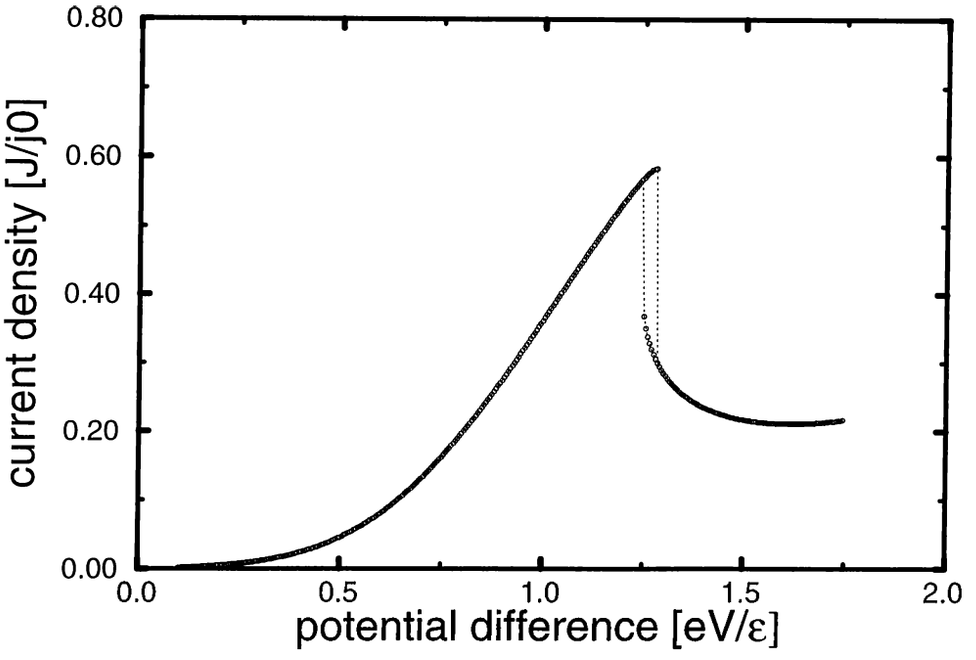

Figure 4.7: Bistable behavior.
Current versus applied bias for four particles

In all the results that will be shown hereafter, energy is scaled with $\epsilon = \hbar^2/(2md^2)$ with $2d$ being the distance between the barriers. Time scale is $t_0 = \hbar/\epsilon$, current density is also scaled relevantly with j_0.

In Fig. 4.5 and Fig. 4.6, current densities versus applied bias of the double barrier structure in the mean field approximation is drawn for four and eight particles respectively. In these two figures the curves correspond to an increasing interaction constant as the peak of the curves goes left to right. At the right most curves bistable behavior is visible.

The curve that exhibit bistability for the given interaction constant is drawn in Fig. 4.7 for four particles. Corresponding curve for eight particles is not drawn but in Fig. 4.8 it is shown that they do not differ much. In Fig. 4.7 lower curves for a given bias are found using initial guess wave-functions which are zero interaction wave-functions and/or which are solutions of the problem for a bias slightly greater than the actual value. Upper curves for a given bias are

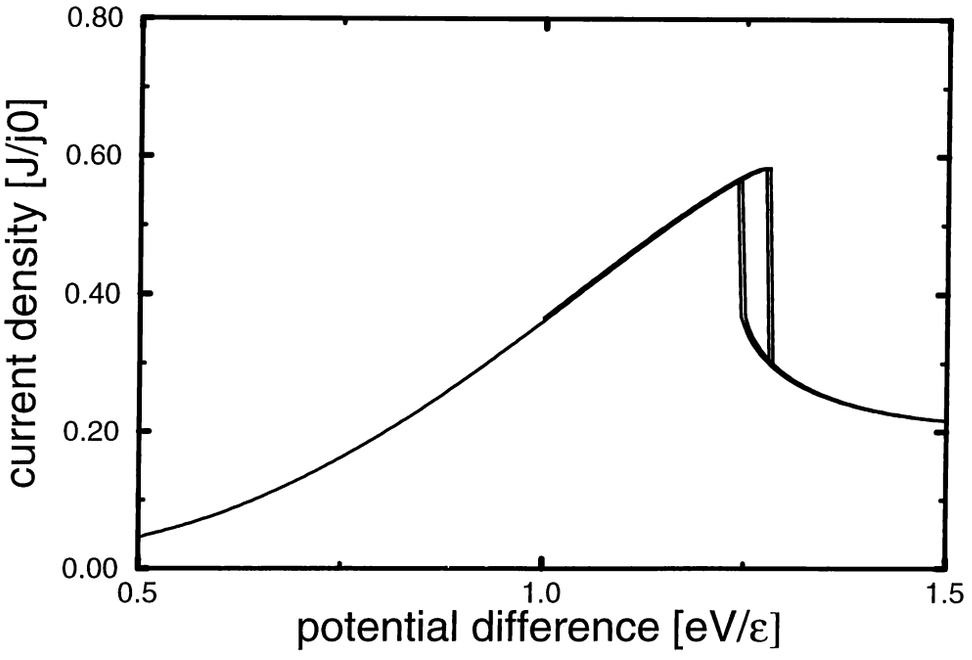

Figure 4.8: Testing the convergence
Four and eight particles results are shown in the bistable region.

found using initial guess wave-functions which are solutions of a bias slightly less than the actual value and/or solutions of the problem for an interaction strength greater than the actual value. Note that for each interaction four types of initial guesses are used and each curve correspond to two different initial guesses.

When the solutions of the double barrier structures are built up in the next sections, two type of methods methods for the time-dependence of the interaction are used in relation to this problem. First, an adiabatic increase in the interaction strength, which may correspond to zero interaction initial guess in this problem.The second approach is to increase the interaction strength adiabatically to a value greater than the actual value and then lower it to its actual value. This may correspond to an initial guess which is a solution of the problem for an interaction strength greater than the actual value.

The switching of the value of the wave-function at an arbitrary point for increasing bias is drawn in Fig. 4.9. Here x axis is the number of iterations

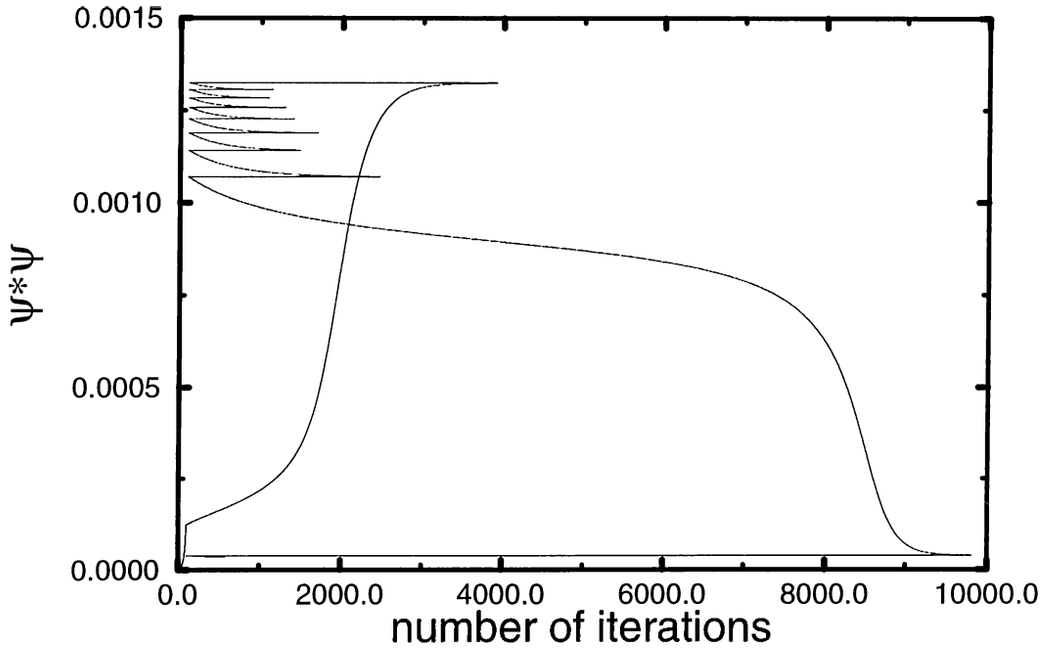

Figure 4.9: Switching of the value of the wavefunction.

performed. The switching from the upper curve to the lower curve is the longest path in the figure that combines the two line segments. It is seen that as the bias increases the number of iterations to find the wave-function increases and at some bias it suddenly increases rapidly and then begin to decrease.

Finally, to understand if the solution is converging to an actual many body problem, the comparison of four and eight particle results are given in Fig. 4.8. It is seen in this figure that different particle numbers corresponds nearly the same curves, as a result it can be concluded that it converges.

4.5 Application of the method

In the simple model of DBRT shown in Fig. 4.2, the Schrödinger equation for single particle states are solved exactly. Considering only regions II,III, and IV in Fig. 4.2, it is clear that for a wave incident from left, solution can be written

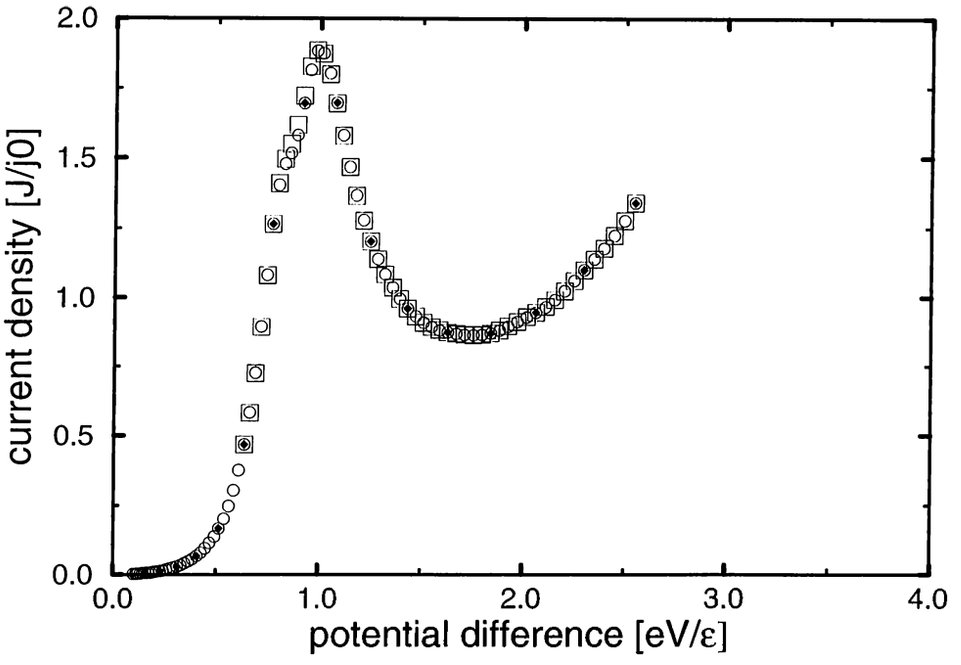

Figure 4.10: Possible error sources of the numerical study Parameters are described in the text.

trivially as:

$$\psi(x) = \begin{cases} e^{iqx} + re{-}iqx & \text{in region II} \\ Ae^{iqx} + Be^{-iqx} & \text{in region III} \\ te^{iqx} & \text{in region IV} \end{cases} \tag{4.11}$$

Completeness and orthogonality of these solutions are obvious since the total Hamiltonian is Hermitian.

As described in the previous chapter q values are discretized such that:

$$q = k\Delta q \tag{4.12}$$

with $k = \cdots, -2, -1, 0, 1, 2, \cdots$.

Positive momentum represents a wave incident from left and negative momentum represents a wave incident from right. Transmission probability versus energy of the wave incident from left for various barrier heights, for zero electron-electron interaction is drawn in Fig. 4.3. After the discretization process,

an upper bound for the energy less than the energy of the second resonance is selected. For example $E = 4\epsilon$ is convenient for this transmission property.

It was shown in the previous chapter for the test geometry that by excluding the states whose energy are far from the energy of the incident state from the basis functions does not introduce an appreciable error to the result. For the double barrier structure, the many particle states whose energy are far from the energy of the incident state are also excluded from the basis. Of course this exclusion reduces the precision of the results but it will be shown later in Fig. 4.10 that the error due to this exclusion is negligible. The states whose energy are in the ΔE neighborhood of the incident state are in the basis.

In the discretization of the time steps, Δt is used as the time between two consequetive calculations of the wave-function in time. Time-dependence of the interaction strength is given in Fig. 3.2.

4.5.1 Results

$\Delta q/\sqrt{2m\epsilon/\hbar}$	0.001	0.001	0.001	0.01	0.01	0.01
$\Delta E/\epsilon$	0.1	0.2	0.01	0.1	0.1	0.2
$\Delta t\epsilon/(\pi\hbar)$	1/15000	1/15000	1/10000	1/15000	1/10000	1/10000
E_{upper}/ϵ	5	5	4	4	5	4

Table 4.1: Parameters explained in the text.

Mainly there are three types of error sources. Discretization procedure for the spectrum of non-interacting Hamiltonian and time steps, putting an upper bound for the energy of the wave-functions that are included in basis and, excluding the wave-functions whose energy are far from the energy of the incident state. In Fig. 4.10, there are six different graphs corresponding to same interaction in the region of interest of parameters that are shown in Table. 4.1. It is appearent that in the region of interest of these parameters, the error is negligible.

Based on the results shown in Fig. 4.10, the following parameters were used in this work.

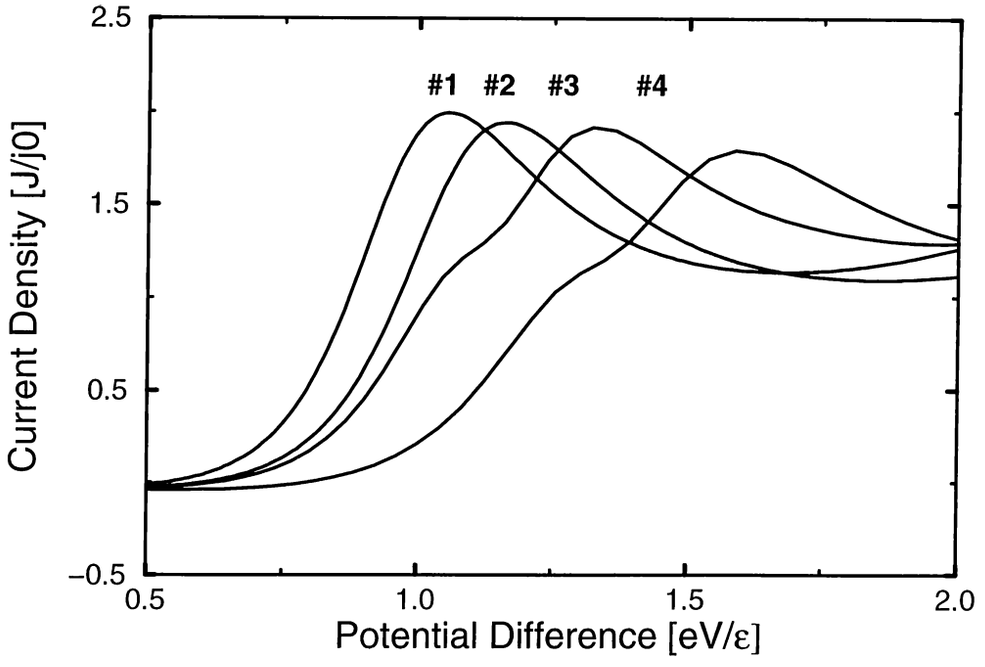

Figure 4.11: Two particle current versus potential difference for β equals 0, 0.001, 0.002, and 0.0025 times ϵ from left to right respectively.

$$\begin{cases} \Delta q & = 0.01\sqrt{2m\epsilon}/\hbar \\ \Delta E & = 0.1\epsilon \\ \Delta t & = \frac{\hbar\pi}{15000\epsilon} \\ E_{upper} & = 4\epsilon \end{cases} \tag{4.13}$$

In Fig. 4.11 current density versus potential difference is drawn for 2 particles. Same for four particles is drawn in Fig. 4.12. The curves corresponds to an increasing interaction constant as we go from left to right. The values of the interaction constants are determined using the results of mean-field approaches. In the figure interaction constants are zero, 0.001, 0.002 and 0.0025 times ϵ. As the interaction constant increases the curves begin to broaden and there is some structure at the left sides of tops of rightmost two curves. This may be due to the inadequacy of the numerical approach, or may be due to the large accumulation of the charges near the resonant energy.

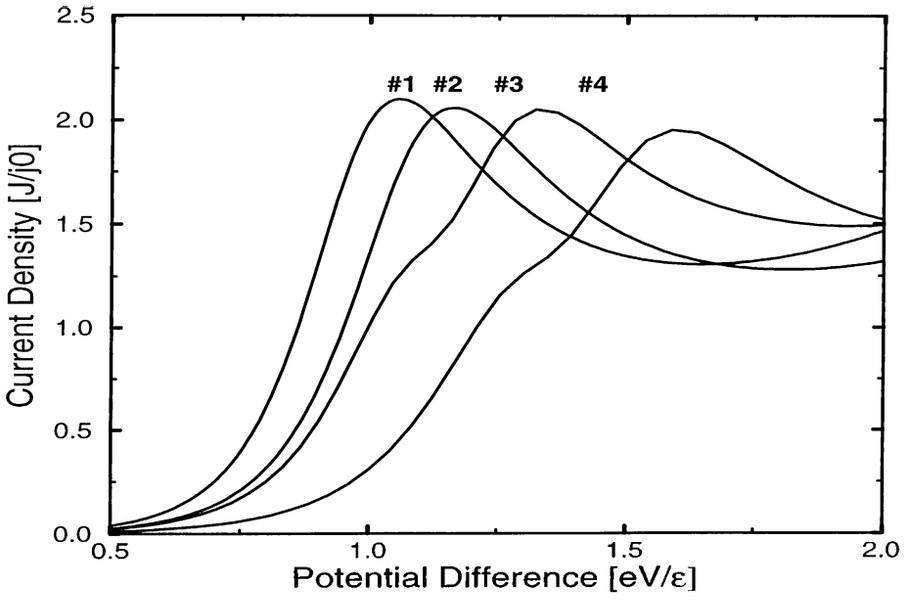

Figure 4.12: Four particle current versus potential difference for β equals 0, 0.001, 0.002, and 0.0025 times ϵ from left to right respectively.

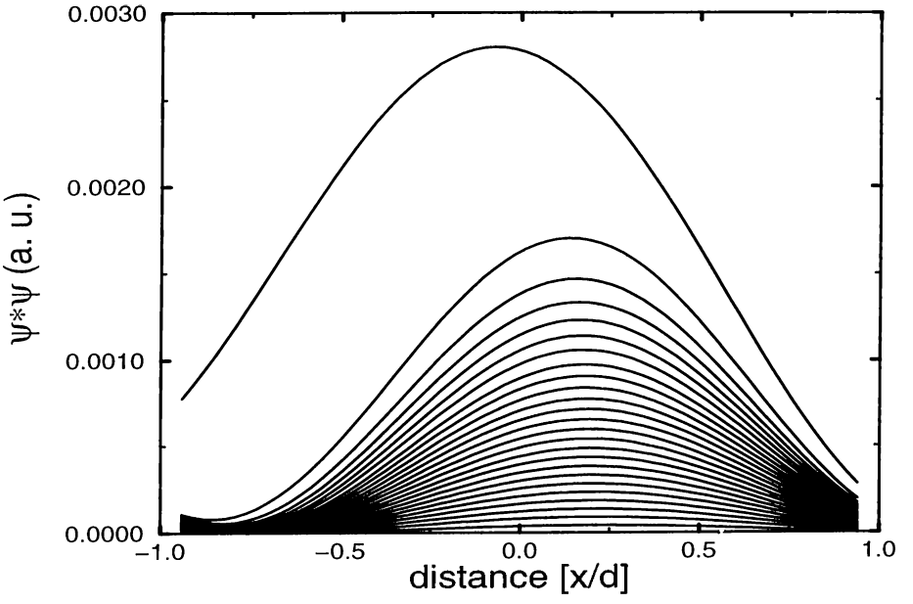

Figure 4.13: Wave-function between the barriers.
The interaction constant increases from bottom curve to top curve.

As mentioned earlier, in a linear approach it is mathematically impossible to

observe the bistability, but by examining the behavior of the wave-function in the NDR region, one can obtain information about the bistability. The wave-function between the barriers is drawn in Fig. 4.13. Here the curves from bottom to top correspond to wave-functions for increasing interaction constants. Strength of the interaction constant was changed uniformly throughout. It can be seen that the wave-function changes uniformly as the strength of the interaction constant is changed but at some point, it abruptly changes to a very different form. This result may be concluded as there are at least two stable solutions to the problem in a specific strength of the interaction constant, probably corresponding to two or more quantum well typed potential seen by the particles.

Consider simply two coupled quantum wells. What happens in time when we drop a particle to one of them is that the probability of finding the particle in any one of the wells oscillate. In Fig. 4.14 for different types of time-dependence of the interaction strength (which corresponds to different initial guesses in mean-field problem) the time-dependence of the current at a particular bias in the NDR region is drawn. Corresponding time-dependences are shown in Fig. 4.15. It is seen from Fig. 4.14 that there are instabilities in the solution, which may be interpreted as transitions between coupled quasi-stable solutions of the system.

In Fig. 4.16 time-dependencies of the wavefunction for two different interaction strengths are drawn. Corresponding values of the strengths are 0.0029 and 0.0025 times ϵ from top to bottom curve respectively. It is clear that the oscillations that are seen in the lower curve no longer exist in the upper curve. The lower curve is the current density at a bistable value, where upper curve is the current density at an interaction slightly above the bistable value.

In Fig. 4.17, six particle results of current voltage graphics are drawn for interaction strengths 0, 0.0015, and 0.0025 times ϵ in order of peak values from left to right. In Fig. 4.18 and Fig. 4.19 oscillations and corresponding time-dependence of the interaction strengths are drawn again for six particles in the NDR region and for an interaction strength where bistability is expected.

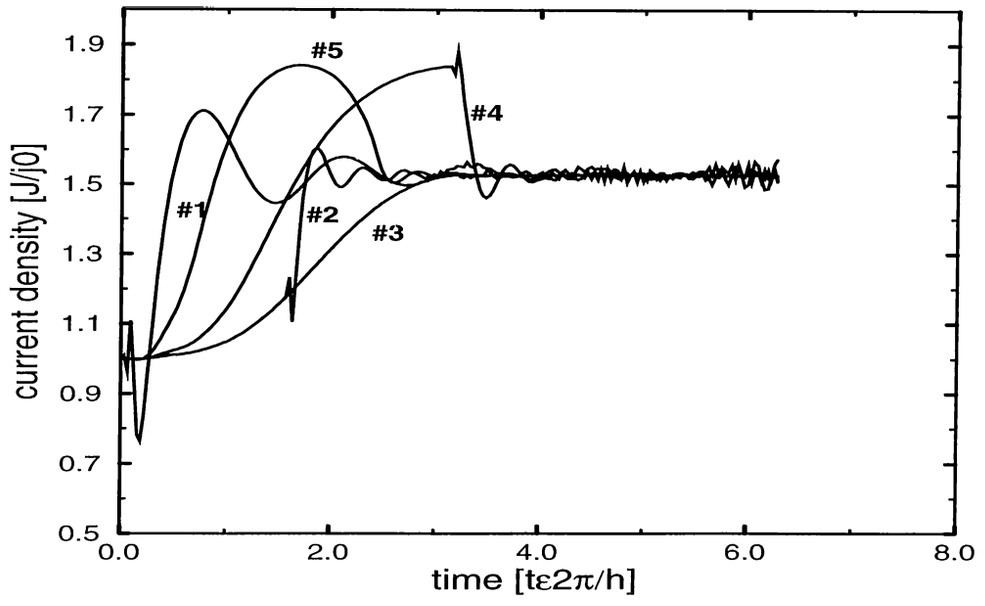

Figure 4.14: Current versus time.
Current calculated at a bias in the NDR region.

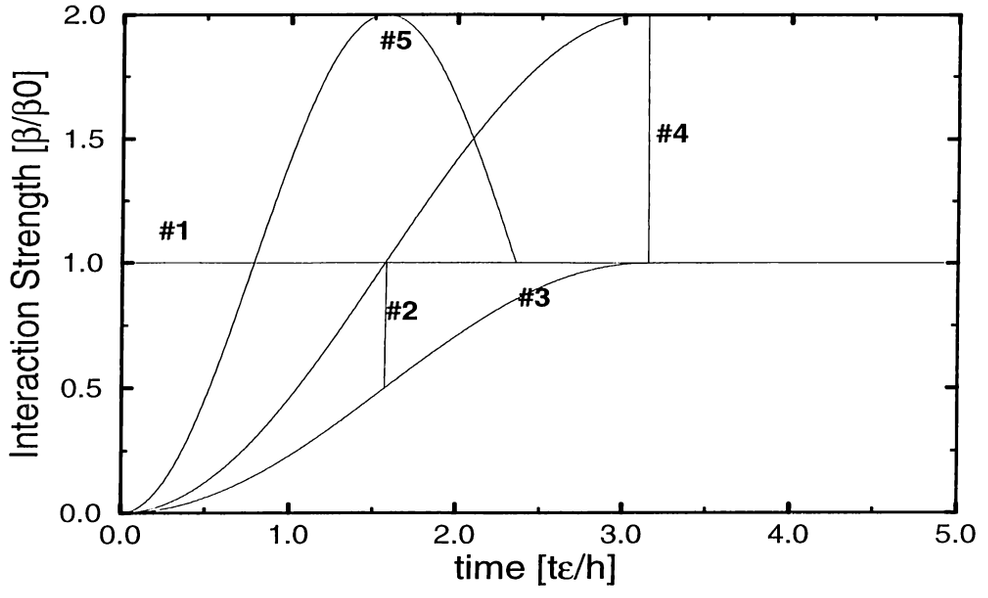

Figure 4.15: Time-dependence of the interaction strength corresponding to previous figure.

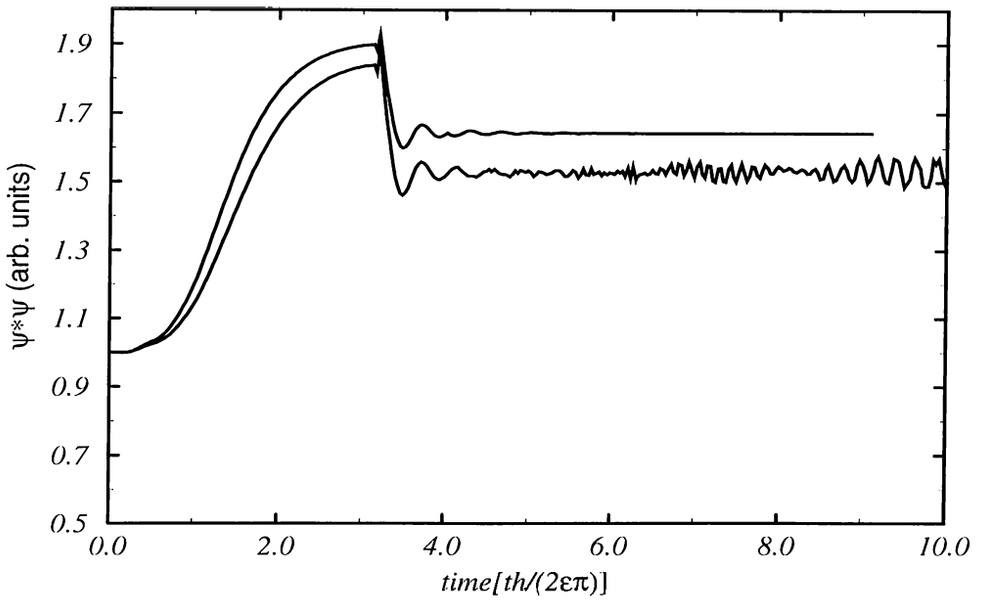

Figure 4.16: Time-dependence of the wave-function for two different interaction constants. Upper curve is for β equals 0.0029, and 0.0025 times ϵ from left to right respectively.

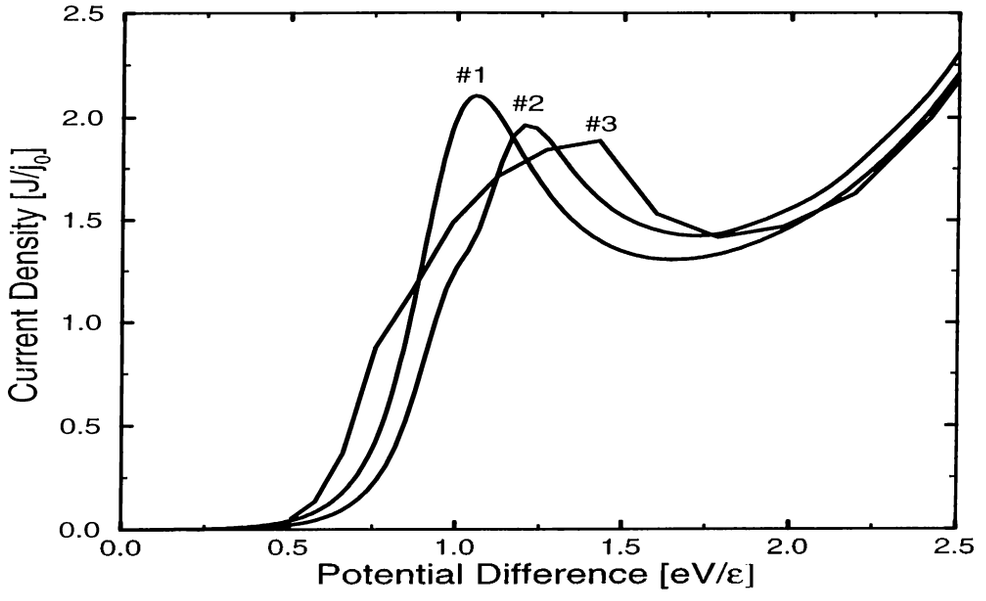

Figure 4.17: Six particle current versus potential difference for β equals 0, 0.0015, and 0.0025 times ϵ from left to right respectively.

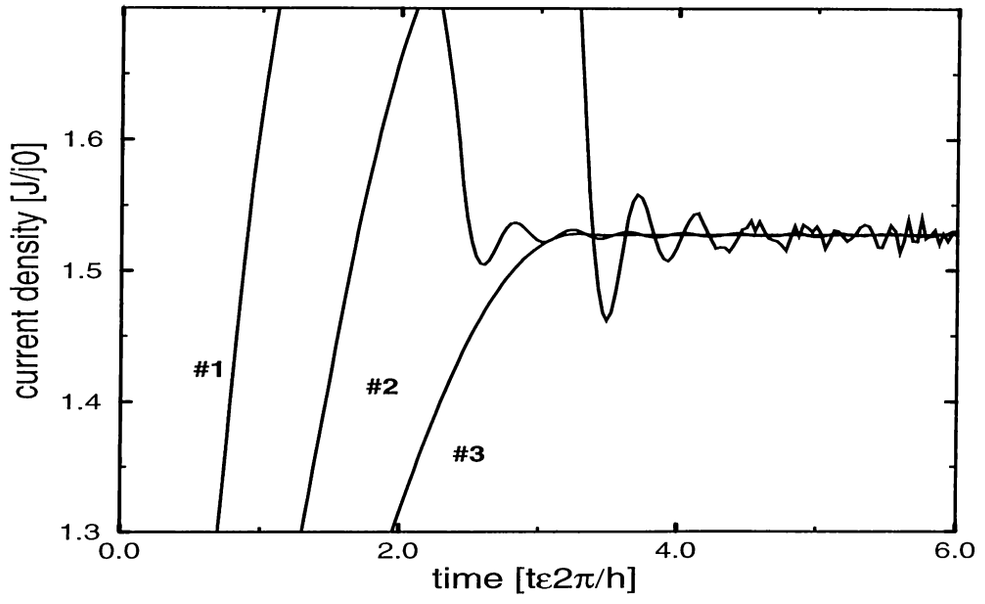

Figure 4.18: Six particle current versus time.
Current calculated at a bias in the NDR region.

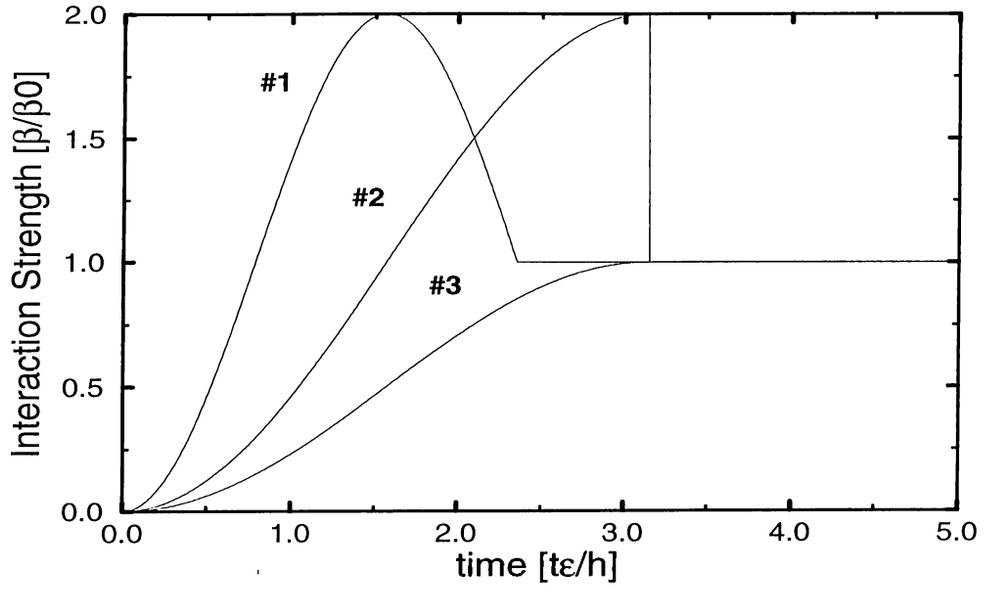

Figure 4.19: Time-dependence of the interaction strength corresponding to previous figure. Six particle results are drawn.

Chapter 5

CONCLUSION

In this thesis, a computational approach based on discretizing the spectrum of the non-interacting Hamiltonian for the study of quantum transport in small systems in the many body picture was proposed. The method mainly depends on discretizing the spectrum of the non-interacting Hamiltonian, choosing an easy representation for the many body picture to include inter-particle interactions, and integrating the time-dependence of the wave-function again in discrete time steps. The computational method proposed is a pure linear quantum mechanical treatment.

The method was tested for a single barrier structure, and it was shown that the results fit well with the exact results. As it is well known, single delta fuction type potentials cause discontinuities in the derivative of the wave-function. The time-dependent method that was proposed handles the problem well and the solution is an excellent approximation to the exact result. Finally, the problem was analysed for different barrier heights. For all different heights, the results always were in good aggreement with the exact ones.

As a second step, a simple model for analysing the bistability in double barrier resonant tunneling structures was constructed. A very simple model was chosen because our aim was to solve the Schrödinger equation exactly when the inter-particle interaction was not present. In order to use such a simple model, it should be somehow shown that this model exhibits bistable behavior. To show

that there exists bistability in these structures, a method depending on solving the self consistent equations of mean field approach was used. This method simply depends on solving the coupled, nonlinear Hartree-Fock equations in an iterative algorith self consistently. Using an iterative algorithm, it was shown that bistability indeed exists in the model that was proposed. The behavior of the model for different strengths of the interactions between particles were analysed. As a last remark it was shown that the problem converges to many body result as the number of particles included are increased.

Finally, the computational method that was proposed to solve the time-dependent Schrödinger equation for the many-body interacting systems (which is exact apart from the discretizations) was applied to the simple model of double barrier resonant tunneling structures. Main difficulties of the application of the method to the geometry arises from the large number of many particle states. When calculating the inter-particle interaction, many states should be included which consumes a large amount of computer time and storage. Inadequate computational resources has reduced the size of simulations that are performed. We believe that with faster and more powerful computers, it will be possible to include more states in the basis so that the numerical approach would sufficiently converge to the continuous case, and more precise results would be obtained.

The behavior of the system under the conditions where bistability is expected (from a mean-field approximation) is studied in detail using the computationally exact many-body method. The simulations were performed for two, four and six interacting particles. Also the problem was simulated for different strengths of the interaction between particles. Our basic aim was to observe bistability in the current-voltage characteristics in a linear approach. Instead oscillations of the current-voltage characteristics in time were observed. This was interpreted as transitions between coupled quasi-stable solutions of the system. To observe the oscillations different types of time-dependencies for the inter-particle interactions were used. It was shown that outside the bistable region (expected from the mean-field approach) there do not exist such similar oscillations.

Considerable improvements on our results are possible: The computations

can be performed for many different parameter settings and larger number of particles, which was not possible for us in the restricted time with the capacities of existing computers. The computational method described in this thesis may be applied to different geometries for the analysis of various many-body interacting systems.

Bibliography

[1] L. L. Chang, L. Esaki and R. Tsu, Applied Physics Letters **24**, 593 (1974).

[2] L. Esaki and R. Tsu, IBM Journal of Research and Develpment **14**, 61 (1970).

[3] R. Tsu, L. Esaki, Applied Physics Letters **22**, 562 (1973).

[4] W. Pötz, Journal of Applied Physics **71**, 2297 (1991).

[5] D. L. Woolard, F. A. Buot, D. L. Rhodes, X. J. Lu, R. A. Lux, and B. S. Perlman, Journal of Applied Physics **78**,1515 (1995).

[6] G. A. Sai-Halasz, M. R. Wordeman, D. P. Kern, S. Rishton and E. Ganin, IEEE Electron Device Letters **9**, 464 (1988).

[7] G. Bernstein, D. K. Ferry and E. Newman, IEEE Electron Device Letters **10**, 444 (1986).

[8] J. Han, D. K. Ferry and E. Newman, IEEE Electron Device Letters **11**, 209 (1990).

[9] B. Kramer and J. Masek, Z. Physik B **76**, 457 (1989).

[10] D. J. Thouless, Physical Review Letters **39**, 1167 (1977).

[11] For a full discussion of Boltzman transport equation see for example, Solid State Physics, N. W. Ashcroft and N. D. Mermin, HRW International Editions, Chapter 16 (1976) or any other textbook on the subject.

[12] M. A. Reed, ed., Nanostructurel Systems, Academic Press, New York (1992).

[13] H. A. Carderia, F, Guinea Lopez and U. Weiss, eds., Quantum Fluctuations in Mesoscopic and Macroscopic Systems, World Scientific Press, Singapore (1990).

[14] B. L. Altshuler, P. A. Lee and R. A. Webb, eds., Mesoscopic Phenomena in Solids, North-Holland, Amsterdam (1991).

[15] H. Fukuyama and T. Ando, eds., Transport Phenomena in Mesoscopic Systems, Springer-Verlag, Tokyo (1992) .

[16] Y. Imry, Europhys Letters **1**, 249 (1986).

[17] R. A. Webb, S. Washburn, C. P. Umbach and R. B. Laibowitz, Physical Review Letters **54**, 2696 (1985).

[18] Y. Aharonov and D. Bohm, Physical Review **115**, 485 (1959).

[19] Y. Aharonov and D. Bohm, Physical Review **123**, 1511 (1961).

[20] D. V. Averin and K. K. Likharev in [14].

[21] J. R. Barker and D. K. Ferry, Solid State Electronics **23**, 519 (1980).

[22] E. Tekman, *Ballistic Transport and Tunneling in Small Systems*, Ph.D. Thesis, Bilkent University (unpublished) (1990).

[23] W. R. Frensley, Reviews of Modern Physics **62**, 745 (1990).

[24] D. K. Ferry and H. L. Grubin in H. Ehrenreich, F. Spaepen, eds., Solid State Physics, Academic Press, New York, pp. 283-448 (1995).

[25] R. Kubo, Journal of Physical Society of Japan **12**, 570 (1957).

[26] D. A. Greenwood, Prooceedings of the Physical Society of London **71**, 585 (1958).

[27] R. Landauer, IBM Journal of Research and Development **1**, 223 (1957).

[28] R. Landauer, Philosophical Magazine **21**, 863 (1970).

[29] M. Büttiker, Y. Imry, R. Landauer, and S. Pinhas, Physical Review B **31**, 6207 (1985).

[30] M. Büttiker, IBM Journal of Research and Development **32**, 317 (1988)

[31] M. Büttiker, Physical Review Letters **57**, 1761 (1986).

[32] W. Kohn and J. M. Luttinger, Physical Review **108**, 590 (1957).

[33] P. N. Argyres and J. L. Siegel, Physical Review Letters **31**, 1397 (1973).

[34] J. L. Siegel and P. N. Argyres, Physical Review **178**, 1016 (1969).

[35] E. Wigner, Physical Reviews **40**, 749 (1932).

[36] L. V. Keldysh, Soviet Physics JETP **20**, 1018 (1965).

[37] L. P. Kadanoff and G. Baym, Quantum Statistical Mechanics, W. A. Benjamin, New York (1962).

[38] J. Rammer and H. Smith, Reviews of Modern Physics **58**, 323 (1986).

[39] G. D. Mahan, Physics Reports **145**, 251 (1987).

[40] G. A. Baker, Physical Review **109**, 2198 (1958).

[41] See for example Y. Isawa in [15] pp.93-99

[42] T. Weil and B. Vinter, Applied Physics Letters **50**, 1281 (1987).

[43] M. İ. Ecemiş, *Time Dependent Study of Quantum Bistaiblity*, Master Thesis, Bilkent University (unpublished) (1995).